



HAL
open science

An X-ray Absorption Fine Structure (XAFS) and Nuclear Magnetic Resonance (NMR) spectroscopy study of gallium-silica complexes in aqueous solution.

Gleb S. Pokrovski, Jacques Schott, Jean-Louis Hazemann, François Farges,
Oleg S. Pokrovsky

► **To cite this version:**

Gleb S. Pokrovski, Jacques Schott, Jean-Louis Hazemann, François Farges, Oleg S. Pokrovsky. An X-ray Absorption Fine Structure (XAFS) and Nuclear Magnetic Resonance (NMR) spectroscopy study of gallium-silica complexes in aqueous solution.. *Geochimica et Cosmochimica Acta*, 2002, 66, pp.(24) 4203-4222. 10.1016/S0016-7037(02)00973-0. hal-00076917

HAL Id: hal-00076917

<https://insu.hal.science/hal-00076917>

Submitted on 31 May 2013

HAL is a multi-disciplinary open access archive for the deposit and dissemination of scientific research documents, whether they are published or not. The documents may come from teaching and research institutions in France or abroad, or from public or private research centers.

L'archive ouverte pluridisciplinaire **HAL**, est destinée au dépôt et à la diffusion de documents scientifiques de niveau recherche, publiés ou non, émanant des établissements d'enseignement et de recherche français ou étrangers, des laboratoires publics ou privés.



An X-ray absorption fine structure and nuclear magnetic resonance spectroscopy study of gallium–silica complexes in aqueous solution

GLEB S. POKROVSKI,^{1,*} JACQUES SCHOTT,² JEAN-LOUIS HAZEMANN,³ FRANÇOIS FARGES,⁴ and OLEG S. POKROVSKY²

¹Institut des Sciences de la Terre d'Orléans (ISTO), CNRS (UMR 6113), 1A rue de la Férollerie, 45071 Orléans cedex 2, France

²Géochimie, Transferts et Mécanismes, CNRS (UMR 5563)-OMP-Université Paul-Sabatier, 38 rue des Trente-Six Ponts, 31400 Toulouse, France

³LGIT and Laboratoire de Cristallographie, CNRS, B.P. 166, 38042 Grenoble, France

⁴Laboratoire des Géomatériaux, Université de Marne la Vallée, 77454 Marne la Vallée cedex 2, France, and Stanford University Environmental Sciences, USA

(Received October 17, 2001; accepted in revised form April 22, 2002)

Abstract—The influence of aqueous silica on gallium(III) hydrolysis in dilute ($2 \times 10^{-4} \leq m_{\text{Ga}} \leq 5 \times 10^{-3}$) and moderately concentrated ($0.02 \leq m_{\text{Ga}} \leq 0.3$) aqueous solutions was studied at ambient temperature, using high resolution X-ray absorption fine structure (XAFS) and nuclear magnetic resonance (NMR) spectroscopies, respectively. Results show that, in Si-free acidic solutions ($\text{pH} < 3$), Ga is hexa-coordinated with oxygens of H_2O molecules and/or OH groups in the first coordination sphere of the metal. With increasing pH, these hydroxyl groups are progressively replaced by bridging oxygens (–O–), and polymerized Ga–hydroxide complexes form via Ga–O–Ga chemical bonds. In the 2.5–3.5 pH range, both XAFS and NMR spectra are consistent with the dominant presence of the Ga_{13} Keggin polycation, which has the same local structure as Al_{13} . Under basic pH ($\text{pH} > 8$), Ga exhibits a tetrahedral coordination, corresponding to $\text{Ga}(\text{OH})_4^-$ species, in agreement with previous NMR and potentiometric studies. Major changes in Ga hydrolysis have been detected in the presence of aqueous silica. Ga is tetra-coordinated, both in basic and acid (i.e., at $\text{pH} > 2.7$) Si-bearing solutions ($0.01 \leq m_{\text{Si}} \leq 0.2$), and forms stable gallium–silicate complexes. In these species, Ga binds via bridging oxygen to 2 ± 1 silicons, with an average Ga–Si distance of $3.16 \pm 0.05 \text{ \AA}$, and to 2 ± 1 silicons, with an average Ga–Si distance of $3.39 \pm 0.03 \text{ \AA}$. These two sets of Ga–Si distances imply the formation of two types of Ga–silicate aqueous complex, cyclic Ga– Si_{2-3} species (formed by the substitution of Si in its tri-, tetra- or hexa-cyclic polymers by Ga atoms), and chainlike GaSi_{2-4} species (similar to those found for Al), respectively. The increase in the number of Si neighbors (a measure of the complex concentration and stability), in alkaline media, with increasing $\text{SiO}_2(\text{aq})$ content and decreasing pH is similar to that for Al–Si complexes found in neutral to basic solutions. At very acid pH and moderate silica concentrations, the presence of another type of Ga–Si complex, in which Ga remains hexa-coordinated and binds to the silicon tetrahedra via the GaO_6 octahedron corners, has also been detected. These species are similar to those found for Al^{3+} in acid solutions. Thus, as for aluminum, silicic acid greatly hampers Ga hydrolysis and enhances Ga mobility in natural waters via the formation of gallium–silicate complexes. Copyright © 2002 Elsevier Science Ltd

1. INTRODUCTION

Although silicic acid, $\text{Si}(\text{OH})_4$, is a major component of natural waters, relatively little attention has been dedicated until recently to its interactions in solution with metals, including aluminum and iron(III). These metals play an important role in a variety of environmental and industrial processes, such as chemical weathering, soil formation or water treatment for purification and consumer use. There is ample evidence that aqueous aluminum/iron(III)–silicate complexes can enhance Al and Fe mobility in aquatic systems. As such, they can exert a significant structural and thermodynamic control on the hydrolysis and condensation reactions of these metals and, thus, on the precipitation of oxides and clay minerals (e.g., Olson and O'Melia, 1973; Schwertmann and Thalmann, 1976; Farmer et al., 1977, 1979; Winters and Buckley, 1986; Decarreau et al., 1987; Birchall et al., 1989; Vempati and Loeppert, 1989; Browne and Driscoll, 1992; Exley and Birchall, 1992, 1993; Xu and Harsh, 1993; Konhauser and Ferris, 1996; Mayer and

Jarrell, 1996; Doelsch et al., 2000). During the last years, different techniques including solubility measurements, potentiometric titrations and spectroscopic analyses were combined to establish the nature, structure and stability of the aqueous complexes formed between Al or Fe and silicic acid (Farmer and Lumsdon, 1994; Pokrovski et al., 1996, 1998, 2001; Salvi et al., 1998; Gout et al., 1999, 2000; Doelsch et al., 2000). The aim of the present work is to combine ^{71}Ga NMR and Ga K-edge XAFS measurements to characterize the local environment around Ga in dilute aqueous solutions with various Si/Ga ratio values and over a wide range of pH.

Because both Ga and Al are located in the third column of the Periodic Table, they exhibit many similar chemical properties, and often close geochemical behavior. The general features of Ga and Al hydrolysis and polymerization in aqueous solution are also similar (Baes and Mesmer, 1976). With increasing pH, both metals hydrolyze with progressive formation of $(\text{Al,Ga})\text{OH}_{1-3}$ monomeric species (Bénézeth et al., 1997; Diakonov et al., 1997), and polymeric polycations at slightly acid pH leading to the precipitation of Al and Ga oxy-hydroxides. At neutral and basic pH, these phases easily dissolve by forming $\text{Al}(\text{OH})_4^-$ and $\text{Ga}(\text{OH})_4^-$ species, respectively. Struc-

* Author to whom correspondence should be addressed (gleb@cnrs-orleans.fr).

tural aspects of Ga hydrolysis, especially in the presence of aqueous silica, are however poorly known. Knowledge of Ga and Al coordination and local atomic environment in their hydroxide and silicate complexes is necessary for understanding the mobility of these metals, the formation of their minerals, and the role of aqueous silica in these processes.

In many studies dealing with the aqueous speciation of aluminum and gallium, nuclear magnetic resonance (NMR) was the chosen spectroscopic method due to its sensitivity to changes in the coordination of these elements, and it has provided clear evidence for the formation of polymeric species in which Al or Ga are both tetra-, and hexa-coordinated (e.g., Akitt et al., 1972; Akitt and Elders, 1988; Thomas et al., 1993; Faust et al., 1995; Öhman and Edlund, 1996; and references therein). However, because both metals exhibit broad NMR resonances in aqueous solution, the assignment of the octahedral signal provided by their monomeric and polymeric complexes is uncertain. X-ray absorption fine structure (XAFS) spectroscopy is the only direct *in situ* method which can provide quantitative information at the atomic scale about the local structural environment of metals in any system, including their aqueous complexes (ligand's identity and number, and inter-atomic distances). Although XAFS spectroscopy of Al (atomic weight 27) is at present limited to high concentrations (>0.1 m), gallium (atomic weight 70) can be studied by XAFS spectroscopy at concentrations as low as 10^{-5} – 10^{-4} m using the third generation synchrotron sources. Although such concentrations are higher than those usually encountered for Ga in natural waters, they are low enough to significantly slow down Ga polymerization and precipitation, and to allow the accurate characterization of Ga–Si interactions (complexation) which can be easily masked by Ga–Ga condensation and solid phase precipitation at higher concentrations. Therefore, XAFS results obtained for Ga–Si interactions can be used for understanding the behavior of this trace element in natural waters. Such data are also believed to produce useful analogies for better understanding Al–Si complexation, based on the similar chemical behavior of Al and Ga. The combination of the ^{71}Ga NMR and Ga *K*-edge XAFS spectroscopic measurements presented in this study provides new insights into the structure of the aqueous species that form during gallium hydrolysis in the presence of silicic acid.

2. MATERIALS AND METHODS

2.1. Sample Preparation

Ga-bearing aqueous solutions for XAFS and NMR experiments were prepared by dissolving weighted amounts of hydrated gallium nitrate ($\text{Ga}(\text{NO}_3)_3 \cdot 9\text{H}_2\text{O}$, 99.99%, Aldrich Chemicals) in doubly deionized water (MilliQ system). The water content of the initial salt was checked by analyzing solutions by flame atomic absorption and was found to be close to the theoretical value within 2 wt. %. The pH of the solutions was adjusted by adding 1M nitric acid (HNO_3) or 1M tetramethylammonium hydroxide ($(\text{CH}_3)_4\text{NOH}$) Titrisol solutions, and measured before and after experiment with a combination pH glass electrode (SCHOTT-H61) calibrated on the activity scale using the NIST tartrate, phthalate, phosphate, and borate buffers ($\text{pH}_{20\text{ }^\circ\text{C}} = 1.69, 4.00, 6.87, \text{ and } 9.21$, respectively) and 0.1 m HCl and 0.01 m NaOH solutions ($\text{pH}_{20\text{ }^\circ\text{C}} = 1.11$ and 12.12, respectively). Silicic acid (H_4SiO_4) was introduced in the Ga-bearing solutions as weighted amounts of a 0.67 m Si solution, prepared by equilibration of amorphous silica powder ($\text{SiO}_2 \cdot 2.2\text{H}_2\text{O}$) at ambient temperature in a 0.5 m tetramethylammonium hydroxide solution. Tetramethylammonium and nitrate were cho-

sen in this study as the major cation and anion, respectively, because of their very low complexing affinity for metals in aqueous solution (Baes and Mesmer, 1976; Wesolowski et al., 1995) even in comparison to other commonly used background ions (Na^+ , K^+ , Cl^-). The influence of NO_3^- and $(\text{CH}_3)_4\text{N}^+$ on Ga hydrolysis and Ga–Si complexing in solution can thus be neglected when analyzing XAFS and NMR spectra. To avoid possible polymerization and/or precipitation during sample preparation, solutions were vigorously stirred using a magnetic stirrer, and then immediately filtered through a 0.2- μm Millipore filter. Measurements were performed within 1 to 2 hours after solution preparation. Ga and Si concentrations in the experimental solutions used for XAFS experiments ranged from 0.0002 to 0.005 m and 0.01 to 0.10 m, respectively. For NMR measurements, more concentrated solutions containing 0.02 to 0.3 m Ga and 0.05 to 0.2 m Si were used. The pH of the solutions in both types of experiments ranged from 1 to 11, which correspond to H/Ga and OH/Ga hydrolysis ratios from 100 to 0 and 0 to 4.5, respectively, depending on Ga concentration. Monomeric silica, total Si and total Ga concentrations were determined using the molybdate blue colorimetric method (Koroleff, 1976), ICP–MS (inductively coupled plasma mass spectrometry) (see details in Pokrovski and Schott, 1998), and flame atomic absorption spectroscopy (see Bénézeeth et al., 1997). Analyses performed on solutions before and after XAFS and NMR spectra acquisitions showed no changes in Si and Ga concentrations in the limit of the analytical uncertainties ($\pm 5\%$ of total concentration). Silicic acid remained essentially monomeric ($>90\%$ of total Si) in the alkaline solution after experiments. In acid solutions, silica polymerization occurred rapidly (within several min.), and more than 50% of total Si was found to be polymerized after measurements in the solutions with high aqueous silica concentrations. In some solutions with the highest Si concentration (0.1 m) at near-neutral pH, a silica gel was observed after measurements, depending on pH and time of measurement. However, the structural environment of Ga derived from the XAFS spectra was found to be only slightly sensitive to silica polymerization (see below). No significant pH changes (± 0.1 – 0.2 pH unit) were recorded after experiments for most solutions. Although the majority of solutions at pH higher than 3 were significantly supersaturated with respect to Ga oxy-hydroxides ($\alpha\text{-GaOOH}$, $\text{Ga}(\text{OH})_3$), the constancy of Ga and Si concentrations and pH, measured before and after experiments on solutions filtered through 0.2- μm membrane filters, indicates that no precipitation of Ga phases occurred during measurements. The presence of nanoparticles of these and other solid phases, which could have passed through the 0.2- μm filter, can also be excluded. Such particles would have inevitably introduced fluctuations of Ga concentration on the beam passage through the aqueous sample, so that the resulting X-ray absorption spectrum would have exhibited significant irregularities and much higher noise than that for a homogeneous solution. As it can be seen below, XAFS scans recorded in this study for all solutions (except for 0.0002 m Ga, pH = 5; see Sect. 4.2.1), were similar for each given sample and without suspicious noise and flaws, thus demonstrating that no solid phase formation occurred in the experimental solutions.

2.2. NMR Spectra Acquisition

NMR experiments were performed using a Bruker AH 300 WB spectrometer, equipped with a 10-mm multinuclear probehead. To perform quantitative measurements, 3 mL of solution were placed in a 10-mm inner-diameter glass tube. A 3-mm glass tube filled with D_2O and inserted in the 10-mm tube was used as field-frequency lock. ^{71}Ga one-pulse experiments were performed at 91.49 MHz with a $\pi/4$ pulse duration of 5 μs and a recycle time of 1 s. Between 10^3 and 2×10^5 acquisitions were performed depending on aqueous Ga concentration and the intensity of the signal. A line broadening of 35–50 Hz was applied, and the spectra were referenced to a 0.5 M aqueous solution of $\text{Ga}(\text{NO}_3)_3$ ($[\text{Ga}(\text{H}_2\text{O})_6]^{3+}$). The concentration of the Ga_{13} polycation and ^{67}Ga hydroxide complexes in acid silica-free solutions was determined by filling the 10-mm insert tube with a 0.026 M $\text{Ga}(\text{OH})_4^-$ solution containing D_2O , and by measuring the relative areas of the peaks at 222 [$\text{Ga}(\text{OH})_4^-$], 174 ppm (central ^{141}Ga in Ga_{13} polycation) and 0 ppm (octahedral gallium aquoion and hydroxide complexes). (See Figs. 1 and 2.)

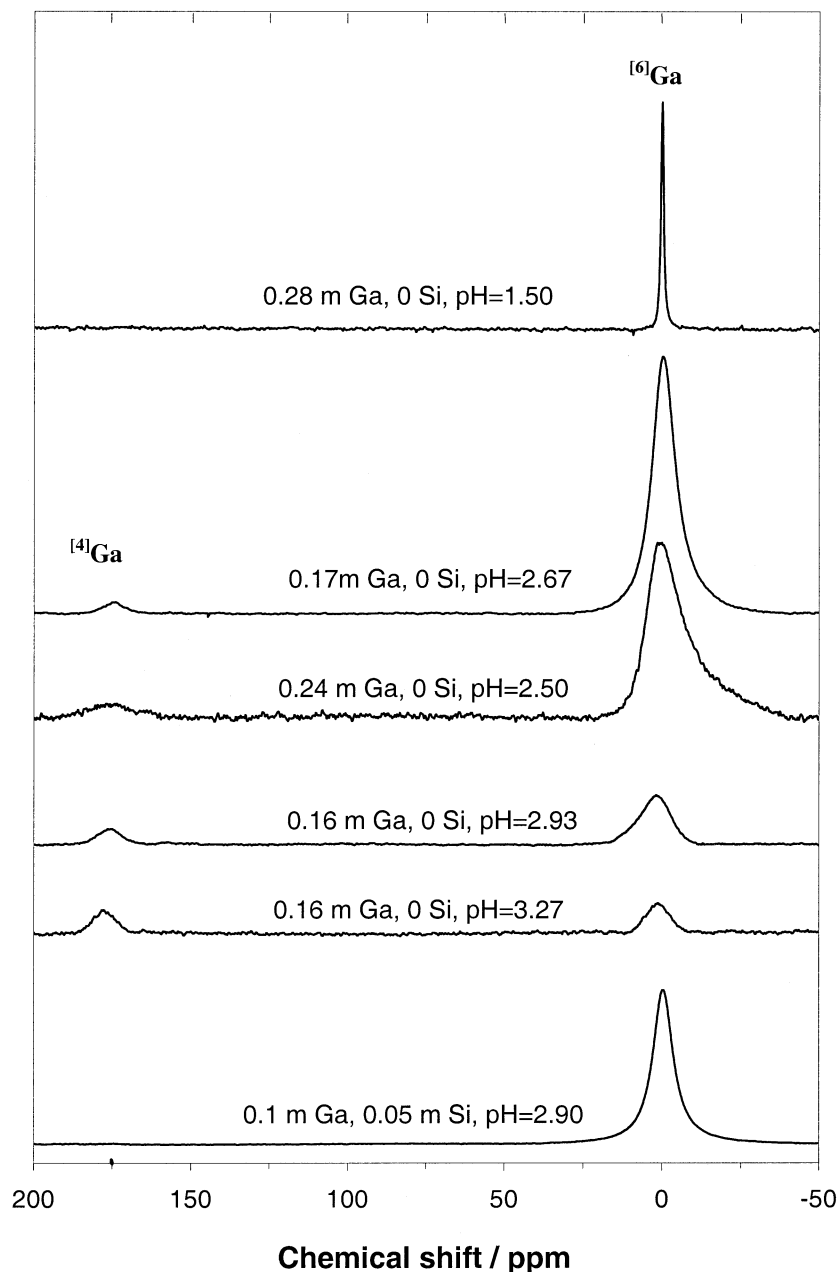


Fig. 1. Evolution of ^{71}Ga NMR spectra of gallium nitrate acid solutions as a function of pH and $\text{SiO}_2(\text{aq})$ concentration. Peaks around 0 and 174 ppm account, respectively, for octahedral and tetrahedral (Ga_{13}) gallium geometry in its aqueous complexes.

2.3. XAFS Spectra Acquisition and Data Reduction

XAFS spectra (including the X-ray absorption near edge structure region or XANES, and the extended X-ray absorption fine structure region or EXAFS) were collected at ambient temperature ($20 \pm 1^\circ\text{C}$) in the fluorescence mode at the Ga K -edge ($\sim 10,370$ eV) over the energy range 10,200–11,800 eV on the collaborative research group IF BM32 beam line at the European Synchrotron Radiation Facility (ESRF, Grenoble, France). The storage ring was operated in the multibunch filling mode at 6 GeV with a 200 mA current. The beam energy was selected using a Si(111) double crystal monochromator with sagittal focussing. The fluorescence spectra were collected using a Canberra 30-element solid state detector. The solutions were placed in a special Teflon cell with kapton-film windows. The cell handling and

spectra acquisition procedure were similar to those described in Pokrovski et al. (2000). In order to obtain the necessary signal-to-noise ratio for quantifying next-nearest neighbors (Ga, Si) around the absorbing Ga atoms, 3 to 6 scans (of ~ 50 min/scan data collection time) for each solution were performed up to high k values ($14\text{--}14.5 \text{ \AA}^{-1}$). After acquisition, all scans for each sample were carefully inspected for each solid state detector and, if found reasonably free of beam intensity fluctuations and other flaws, were added together. Solid gallium hydroxide, $\alpha\text{-GaOOH}$, and nitrate, $\text{Ga}(\text{NO}_3)_3 \cdot 9\text{H}_2\text{O}$, which can serve as model compounds for Ga local environment, were recorded in the transmission mode to exclude self-absorption effects.

XAFS data analysis were performed using the SEDEM (Aberdam, 1998) and XAFS2.6 (Winterer, 1997) packages. Both programs have

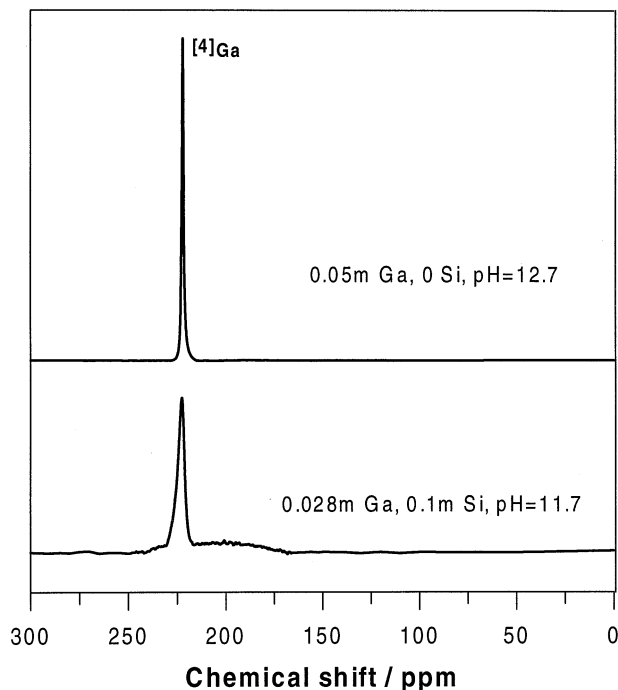


Fig. 2. ^{71}Ga NMR spectra of gallium nitrate basic solutions with and without aqueous silica. The peaks correspond to tetrahedral Ga coordination in its hydroxide and silicate complexes.

produced the same results in the limit of the uncertainties when extracting structural information for the Ga coordination shells (see below). The analysis of the XANES data was performed in the region of 100 eV below and 200 eV above the absorption edge using a procedure similar to that of Farges et al. (1996a). First, the before-edge spectral region (10,200–10,300 eV) was fitted using a Victoreen function and subtracting this as background absorption. Then, the XAFS spectra were normalized for atomic absorption, based on the average absorption coefficient of the spectral region 10,370–10,600 eV. The spectra obtained were superposed to compare the white line position and the shape of peaks for different solutions (e.g., Fig. 3).

EXAFS spectra were analyzed as previously described in Pokrovski et al. (2000), and following the “standard” procedure (Teo, 1986). Energies were recalculated into k space (\AA^{-1}) with E_0 (i.e., the energy where k is zero) arbitrarily chosen at zero of the edge first derivative. The k^2 -weighted EXAFS spectra were Fourier transformed over the k range from 3 to 14\AA^{-1} a Kaiser–Bessel window function (Bonnin et al., 1985) with τ values of 2.5 in order to reduce termination effects in the Fourier transform (FT) (e.g., Figs. 4b and 5b). To extract structural information, one or several FT peaks were back-transformed into momentum space (inverse Fourier transform, IFT) (Figs. 6 and 7). Modeling of these EXAFS oscillations (IFT) by least-square fitting gives average structural parameters for the Ga environment (identity of first and second (if present) neighbor atoms, distances (R) between Ga and their neighbors, average coordination numbers (N), and the Debye–Waller factors (DW, σ^2) which is a measure of disorder). Raw EXAFS spectra were also fitted with multiple shells (Fig. 8); they produced values of structural parameters similar to those extracted from fits of individual IFTs. For most spectra of Ga–Si solutions with weak second and third shell contributions, fits of the total EXAFS spectrum were, however, less stable and exhibited larger uncertainties than those for the individual-shell IFTs. Consequently, the results of the latter fits were considered to be more reliable and they are reported in this study (Tables 1 and 2). Theoretical backscattering amplitude and phase-shift functions for Ga–O, Ga–Ga, and Ga–Si pairs were computed using the FEFF 6.01 *ab initio* code (Ankudinov and Rehr, 1997; Zabinsky et al., 1995), assuming the local structure around Ga in α - $^{161}\text{GaOOH}$ (Pye et al., 1977) and a ^{141}Ga -zeolite, $\text{Na}_3(\text{Ga}_3\text{Si}_3\text{O}_{10})(\text{H}_2\text{O})_4$ (Nenoff et al.,

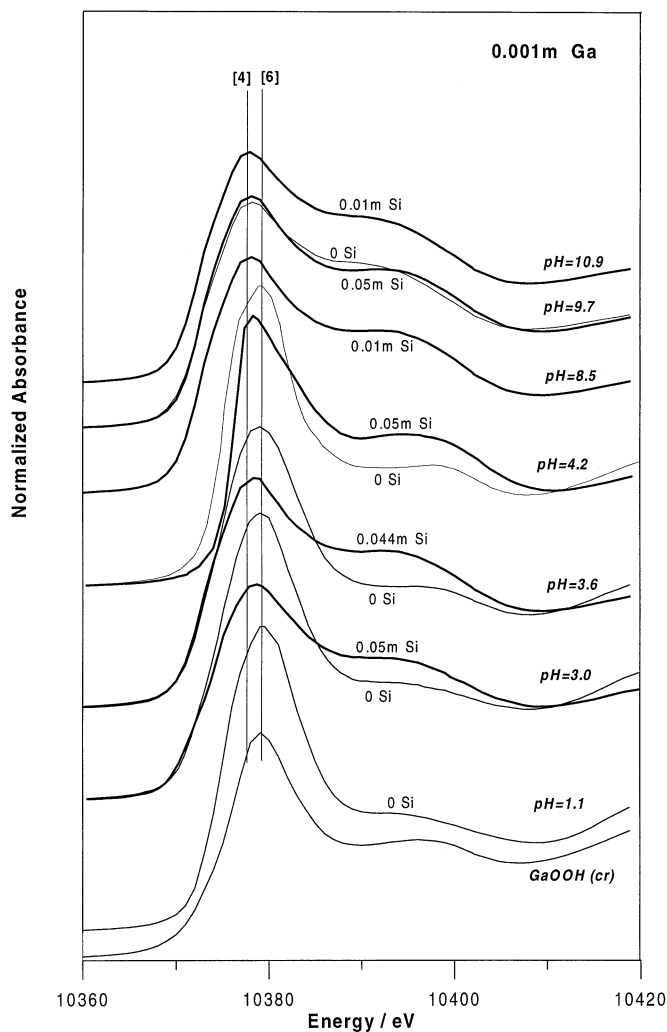


Fig. 3. Normalized XANES spectra of selected 0.001 m Ga nitrate solutions with (thick curves) and without (thin curves) aqueous silica. Vertical lines denote shifts in edge-crest energy corresponding to the octahedral (α -GaOOH and silica-free acid solutions) and tetrahedral (Si-free basic solutions and Si-bearing acid and basic solutions) Ga local geometry.

1994). The amplitude reduction factor S_0^2 and Debye–Waller factors were set to 1 and 0, respectively, in the calculations of these functions. The validity of the calculated amplitude and phase functions was checked by fitting EXAFS spectra of α -GaOOH and $\text{Ga}(\text{NO}_3)_3 \cdot 9\text{H}_2\text{O}$. The influence of possible disorder (thermal and static) in determining structural parameters was checked using an anharmonic approach consisting of adding, in the expression of the pair-correlation function between absorbing element and their neighbors, third- (C_3) and fourth-order (C_4) cumulants accounting for the anharmonicity (Crozier et al., 1988; Farges, 1996; Farges et al., 1996b; Soldo et al., 1998). The typical values of C_3 and C_4 found when fitting our IFT spectra for the Ga first coordination shell were of the order of 10^{-4} , and did not change significantly R and N values derived from least-square fits without cumulants. As a result, in order to reduce the number of variables and thus the uncertainties on the derived parameters, we decided not to use the anharmonic approximation when extracting R , N , and σ values for all Ga atomic shells. The influence of possible multiple scattering phenomena (MS) within the Ga first coordination shell on the EXAFS spectra was also tested using the FEFF code. With the exception of the most acid Ga solutions (pH \sim 1), MS contributions from the

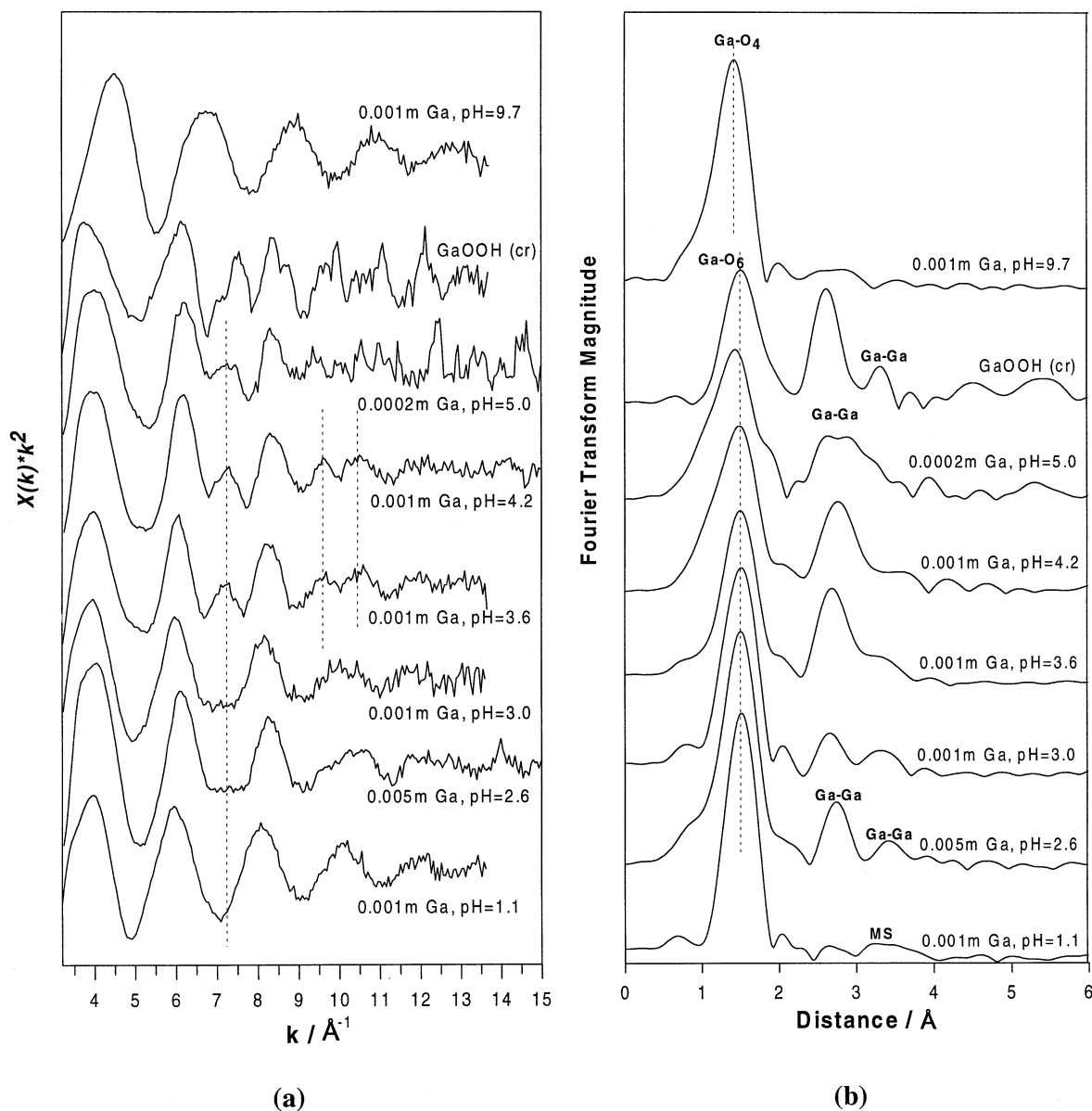


Fig. 4. k^2 -weighted EXAFS spectra at Ga- K edge of selected Si-free Ga nitrate solutions as a function of pH, and α -GaOOH solid (a), and their corresponding Fourier transforms (not corrected for phase shift) (b). The vertical lines on (a) indicate the appearance of new contributions with increasing pH, which correspond to Ga-O-Ga bonds in the polymerized Ga hydroxide complexes. The vertical lines on (b) denote Ga tetrahedral (at basic pH) and octahedral coordination (at acid pH and α -GaOOH).

first shell were found to be negligible when fitting the second and third Ga atomic shells.

3. NMR RESULTS

3.1. Acid Solutions

^{71}Ga NMR spectra of $\text{Ga}(\text{NO}_3)_3$ aqueous solutions ($0.05 \leq m_{\text{Ga}} \leq 0.24$) obtained at different selected pH (different degrees of Ga^{3+} hydrolysis) in the presence or not of aqueous silica are presented in Fig. 1. In strongly acid silica-free solutions (pH ~ 1.5), a single narrow peak (half height width, $W_{1/2H} = 110$ Hz) corresponding to octahedral gallium

$[\text{Ga}(\text{H}_2\text{O})_6]^{3+}$ is observed at 0 ppm. As pH increases and hydrolysis progresses, the octahedral gallium peak broadens markedly (from 100 Hz at pH = 1.5 to 1500 Hz at pH = 3.3) while a small broad peak (~ 1300 – 1600 Hz) located at ~ 174 ppm appears. The peak at 174 ppm corresponds to gallium atoms in a distorted tetrahedral environment and has been assigned to the central gallium atom surrounded by 12 edge-linked Ga octahedra of a $[\text{GaO}_4\text{Ga}_{12}(\text{OH})_{24}(\text{H}_2\text{O})_{12}]^{7+}$ (Ga_{13}) polycation analogous to Al_{13} (Johanson, 1962a, 1962b; Bradley et al., 1990a, 1990b; Michot et al., 2000). It should be emphasized that if this peak is much broader than that of tetrahedral

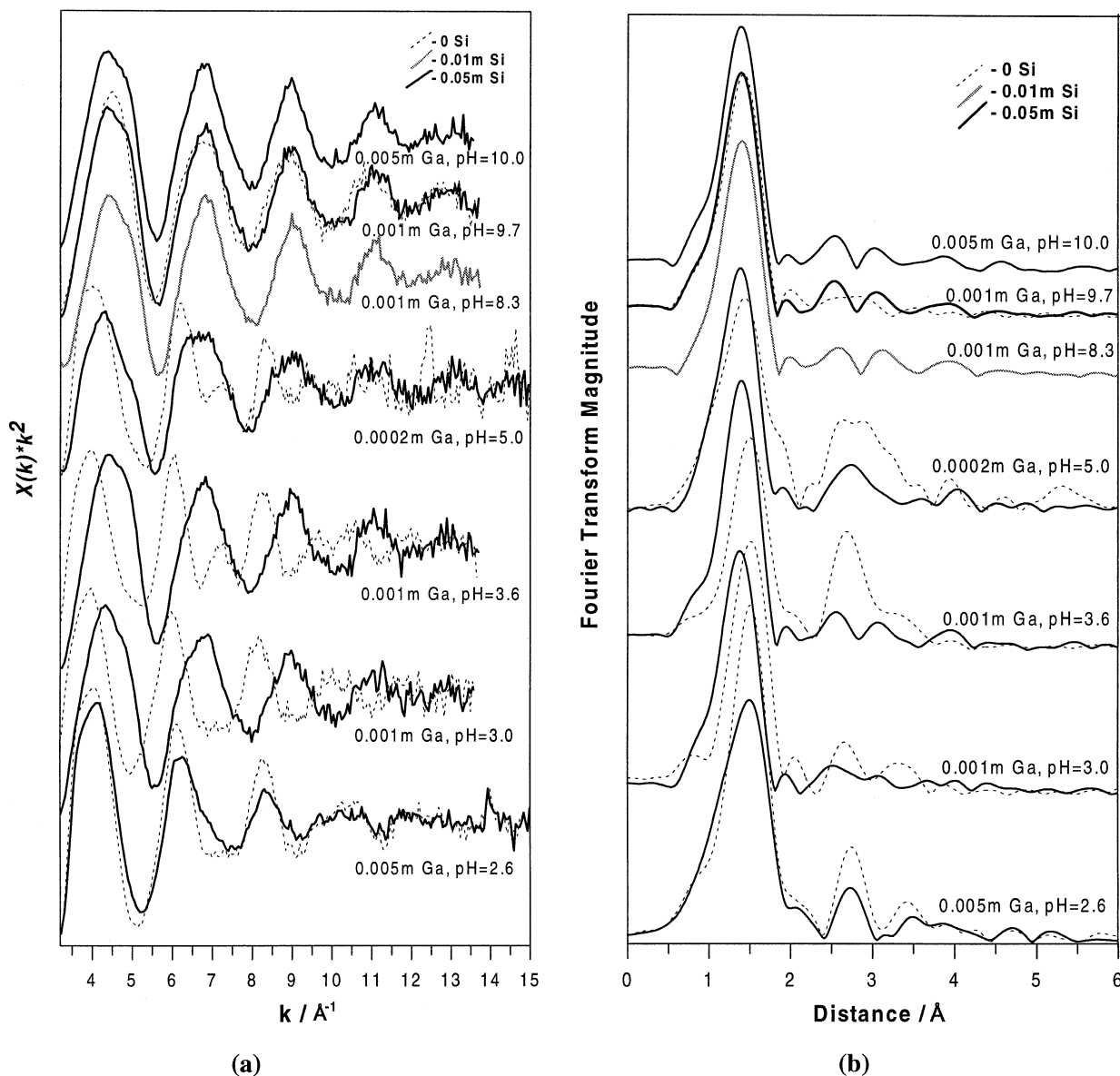


Fig. 5. k^2 -weighted EXAFS spectra at Ga-K edge of selected Ga nitrate solutions in the presence of aqueous silica at different pH (a), and their Fourier transforms (not corrected for phase shift) (b). The solid curves stand for Si-bearing solutions with indicated concentrations, but the dashed curves represent the spectra of the corresponding Si-free solutions at the same pH (see also Fig. 4).

Al in Al_{13} (~ 20 Hz) thus probably reflecting a more distorted environment in the case of tetrahedral Ga, it appears at the exact position expected from the analogy with Al_{13} ($\nu[\text{Ga}_{\text{tetra}}]/\nu[\text{Ga}(\text{OH})_4^-] = \nu[\text{Al}_{\text{tetra}}]/\nu[\text{Al}(\text{OH})_4^-] = 0.78$). The broadening of the octahedral Ga peak at 0 ppm reflects both the presence of Ga monomeric and polymeric hydroxide complexes and the formation of the Ga_{13} polycation. From the relative area of the peaks at 0 and 174 ppm ($S_0/S_{174} \sim 15\text{--}10$) and that of the peak at 222 ppm for the $\text{Ga}(\text{OH})_4^-$ standard solution of known concentration, it can be inferred that the Ga_{13} polycation is largely dominant ($> 60\%$) at $2.5 < \text{pH} < 3.0$. At higher pH, prior to Ga hydroxides precipitation, the ratio S_0/S_{174} decreases

markedly ($S_0/S_{174} \sim 1.6$ at $\text{pH} = 3.3$) which can reflect the hydrolysis of Ga_{13} (i.e., replacement of some of the 12 water molecules by hydroxyl groups) and the subsequent condensation of Ga_{13} species leading to the formation of larger polycations (i.e., " Ga_{26} " or " Ga_{40} ", Baes and Mesmer, 1976) accommodating Ga atoms in both tetrahedral and octahedral coordination (see also XAFS results below). It should be noted that above pH 2.5, as hydrolysis progresses, the surface area of the peak at 174 ppm (compared to that of the $\text{Ga}(\text{OH})_4^-$ standard solution) remains constant whereas that of the 0 ppm peak considerably decreases, so that only $\sim 33\%$ of the Ga initially present in solution could be detected. This suggests that the

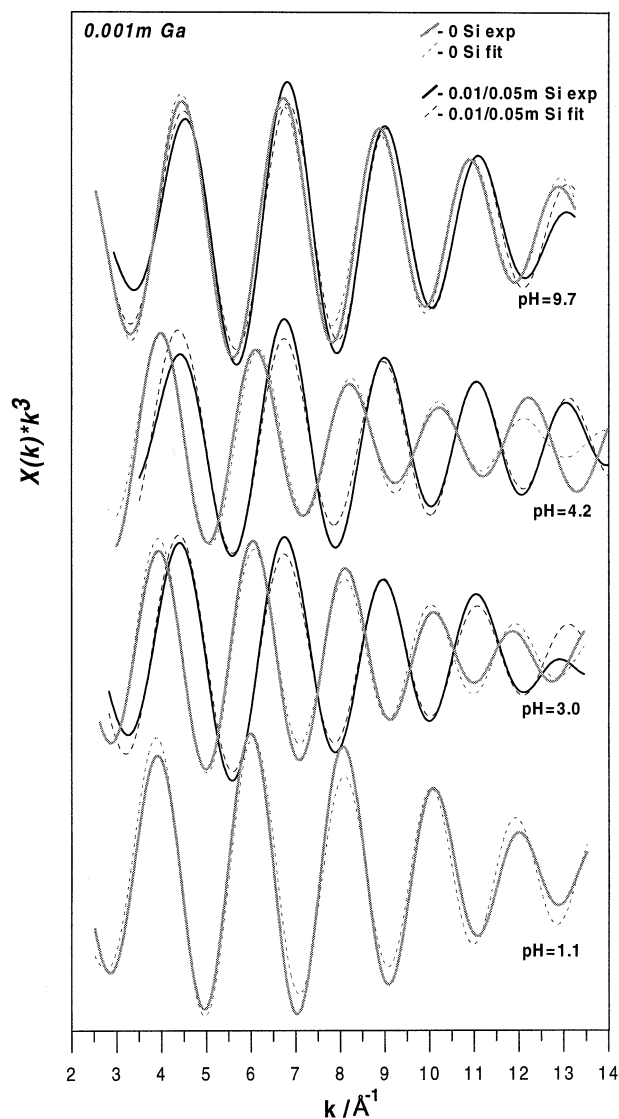


Fig. 6. EXAFS spectra of the first Ga atomic shell of selected 0.001 molal Ga nitrate solutions at indicated pH and Si concentration (solid lines) and their least-square fits (dashed lines). Significant amplitude and phase shifts between acid Si-free and Si-bearing solutions are apparent in this figure. This demonstrates that Ga changes its first shell coordination from 6 to 4 when complexing with silica in acid solutions (see text for details).

octahedral Ga sites in the newly formed polymers could be strongly disordered which attenuates the ^{67}Ga signal; and the tetrahedral Ga sites are likely to have a similar geometry as for the central ^{41}Ga in Ga_{13} . At the same time, careful visual inspection of solutions, and Ga and pH analyses did not allow to detect any precipitation during the NMR measurements.

In silica bearing solutions (e.g., $m_{\text{Ga}} = 0.1$, $m_{\text{SiO}_2(\text{aq})} = 0.05$, $\text{pH} = 2.9$), the octahedral peak broadening considerably reduces ($W_{1/2H} = 690$ Hz) whereas the tetrahedral Ga peak at 174 ppm disappears (Fig. 1). This suggests the formation of aqueous gallium–silica complexes with Ga in sixfold coordination which considerably slow down Ga hydrolysis and prevent the formation of Ga_{13} .

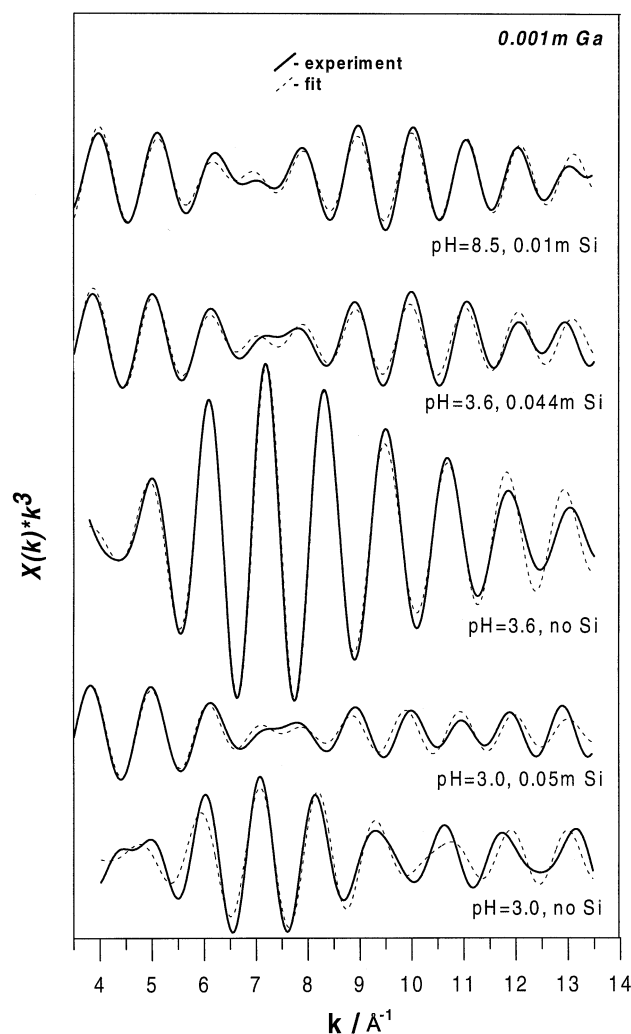


Fig. 7. EXAFS spectra of the second and third Ga atomic shells of selected 0.001 molal Ga solutions at indicated pH and Si concentration (solid lines), and their least-square fits (dashed lines). It can be seen that the amplitude of Ga beyond-the-first atomic shells is significantly suppressed in the presence of silica, which is also accompanied by distinct phase shifts. This demonstrates that the heavy Ga backscatters in the polymerized complexes at acid pH are replaced by lighter silicon backscatters in the presence of aqueous silica (see the text for details and Table 2 for fitted structural parameters).

3.2. Alkaline Solutions

In silica-free solutions ($m_{\text{Ga}} = 0.05$, $m_{\text{SiO}_2(\text{aq})} = 0$, $\text{pH} = 12.7$), a single narrow peak ($W_{1/2H} = 90$ Hz) corresponding to the tetrahedral gallate complex ($\text{Ga}(\text{OH})_4^-$) is observed at 222 ppm (Fig. 2). In the presence of aqueous silica ($m_{\text{Ga}} = 0.03$, $m_{\text{SiO}_2(\text{aq})} = 0.1$, $\text{pH} = 11.7$), this peak broadens ($W_{1/2H} = 410$ Hz), and another very broad feature ($W_{1/2H} = 2450$ Hz) is observed at ~ 195 ppm. The broadening of the 222 ppm peak is a consequence of the exchange of Ga atoms between monomeric gallate and gallosilicate anions (Mortlock et al., 1992). Following Mortlock et al. (1992) and by analogy with the results of ^{27}Al NMR investigation of alkaline aluminosilicate solutions (Pokrovski et al., 1998), the signal at 195 ppm can be

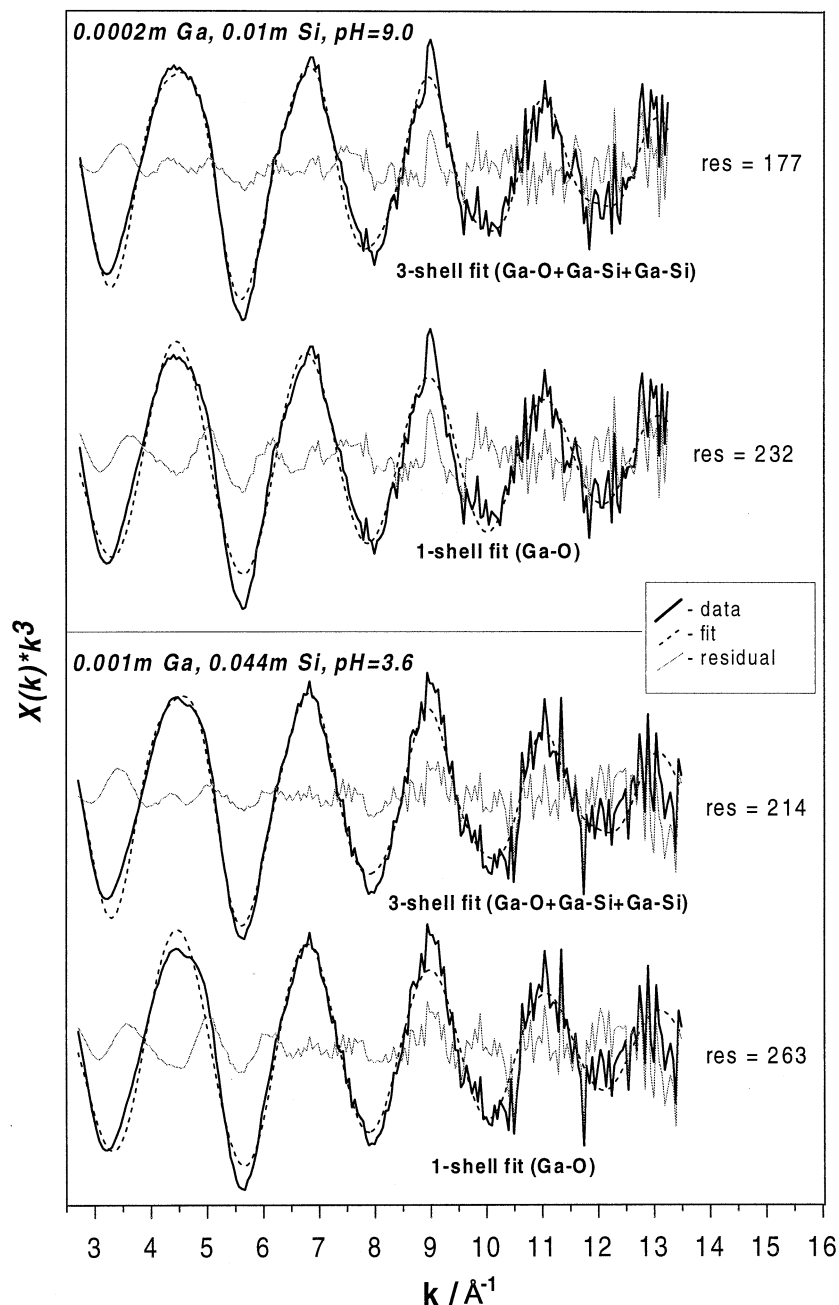


Fig. 8. Example of least-square fits of raw k^3 -weighted EXAFS spectra for selected Si-bearing solutions. Fits were performed with either a single first Ga–O shell or first Ga–O shell plus two outer Ga–Si shells, with parameters (R , N , DW) close to those reported in Tables 1 and 2. It can be seen that adding two Ga–Si contributions significantly improves the fit quality, expressed as $\text{res} = \sum (Y_{\text{data}}^2 - Y_{\text{fit}}^2)$, where $(Y_{\text{data}}^2 - Y_{\text{fit}}^2)$ is the squared difference between experimental and fitted EXAFS absorption coefficient ($K^3 \cdot X$) of the raw EXAFS signal for each point (see also Sect. 4.3.2).

tentatively assigned to Ga atoms in gallosilicate anions with two or three siloxane linkages.

4. XAFS RESULTS

4.1. XANES Analysis

XANES spectra of $\text{Ga}(\text{NO}_3)_3$ alkaline solutions with and without aqueous silica (Fig. 3) exhibit similar shape and edge-

crest positions ($10,378 \pm 0.3$ eV) suggesting the same local structure around Ga in these systems. Available solubility, potentiometric and NMR studies have shown that Ga, like Al, is tetrahedrally surrounded by 4 OH groups in alkaline media (Baes and Mesmer, 1976; Bradley et al., 1990a; Bénézech et al., 1997), which is also confirmed by our NMR measurements (see Sect. 3 above). XANES spectra of silica-free Ga nitrate solutions at pH from 1 to 5 show shapes and edge-crest positions

Table 1. Structural parameters of the first Ga atomic shell obtained from fitting Ga K-edge EXAFS spectra of Ga nitrate solutions with and without aqueous silica.

| Solution composition | | | Atomic pair | R (Å) | N (atom) | σ^2 | chi ² |
|----------------------|-------------|-------------|-------------|---------------|------------|------------|------------------|
| pH | m Ga mol/kg | m Si mol/kg | | | | | |
| 1.1 | 0.001 | 0 | Ga–O | 1.95 (0.01) | 6.0 (0.5) | 0.005 | 1.50 |
| 1.1 | 0.005 | 0 | Ga–O | 1.948 (0.005) | 5.9 (0.2) | 0.005 | 0.54 |
| 2.6 | 0.005 | 0 | Ga–O | 1.940 (0.005) | 6.0 (0.4) | 0.006 | 0.47 |
| 3.0 | 0.001 | 0 | Ga–O | 1.96 (0.01) | 5.5 (0.3) | 0.006 | 1.21 |
| 3.6 | 0.001 | 0 | Ga–O | 1.95 (0.01) | 5.2 (0.5) | 0.007 | 1.10 |
| 4.2 | 0.001 | 0 | Ga–O | 1.94 (0.02) | 5.7 (0.3) | 0.008 | 0.90 |
| 5.0 | 0.0002 | 0 | Ga–O | 1.88 (0.03) | 5.6 (0.3) | 0.009 | 1.07 |
| 9.0 | 0.0002 | 0 | Ga–O | 1.83 (0.01) | 4.0 (0.5) | 0.004 | 1.62 |
| 9.7 | 0.001 | 0 | Ga–O | 1.830 (0.005) | 4.0 (0.3) | 0.0035 | 0.89 |
| 9.6 | 0.005 | 0 | Ga–O | 1.830 (0.005) | 4.0 (0.5) | 0.005 | 1.10 |
| 9.7 | 0.005 | 0 | Ga–O | 1.840 (0.005) | 3.8 (0.2) | 0.0035 | 1.50 |
| 2.7 | 0.005 | 0.056 | Ga–O1 | 1.940 (0.003) | 5.3 (0.4) | 0.007 | |
| | | | Ga–O2 | 1.81 (0.01) | 1.2 (0.2) | 0.006 | 0.60 |
| 2.7 | 0.001 | 0.094 | Ga–O | 1.810 (0.005) | 3.5 (0.5) | 0.004 | 1.06 |
| 3.0 | 0.001 | 0.05 | Ga–O | 1.812 (0.002) | 3.9 (0.2) | 0.007 | 0.73 |
| 3.6 | 0.001 | 0.044 | Ga–O | 1.810 (0.005) | 4.0 (0.2) | 0.004 | 0.70 |
| 4.2 | 0.001 | 0.05 | Ga–O | 1.808 (0.005) | 3.7 (0.5) | 0.004 | 1.25 |
| 5.0 | 0.0002 | 0.05 | Ga–O | 1.81 (0.01) | 3.2 (0.3) | 0.004 | 0.98 |
| 8.2 gel | 0.005 | 0.06 | Ga–O | 1.820 (0.005) | 4.0 (0.3) | 0.004 | 1.70 |
| 8.3 | 0.001 | 0.011 | Ga–O | 1.820 (0.002) | 3.9 (0.2) | 0.004 | 1.40 |
| 8.5 | 0.001 | 0.011 | Ga–O | 1.810 (0.005) | 3.8 (0.3) | 0.003 | 2.00 |
| 9.0 | 0.0002 | 0.01 | Ga–O | 1.810 (0.005) | 4.1 (0.2) | 0.004 | 0.70 |
| 9.7 | 0.001 | 0.01 | Ga–O | 1.805 (0.005) | 3.8 (0.3) | 0.003 | 1.93 |
| 9.7 | 0.001 | 0.051 | Ga–O | 1.807 (0.002) | 4.2 (0.2) | 0.004 | 1.50 |
| 9.7 | 0.005 | 0.05 | Ga–O | 1.810 (0.005) | 3.8 (0.2) | 0.003 | 0.90 |
| 10.0 | 0.005 | 0.048 | Ga–O | 1.812 (0.005) | 4.0 (0.2) | 0.0035 | 1.30 |
| 10.9 | 0.001 | 0.01 | Ga–O | 1.84 (0.01) | 3.8 (0.3) | 0.003 | 1.69 |
| α -GaOOH | | | Ga–O1 | 1.92 (0.01) | 2.5 (0.5) | 0.003 | |
| | | | Ga–O2 | 2.05 (0.02) | 3.0 (0.5) | 0.003 | 0.70 |

R = Ga–neighbor mean distance, N = Ga coordination number, σ^2 = squared Debye–Waller factor, $\text{chi}^2 = D/(F \times M) \times (Y_{\text{exp}}^2 - Y_{\text{fit}}^2)$, where D = number of independent data, F = degrees of freedom, M = number of data points fitted, and $Y_{\text{exp}}^2 - Y_{\text{fit}}^2$ = squared difference between experimental and fitted EXAFS absorption coefficient ($k^3 \cdot X$) of the filtered signal for each point (Press et al., 1986).

Values in parentheses represent average uncertainty for R and N . Typical uncertainty for σ^2 is $\pm 0.0005 \text{ \AA}^2$; gel = the formation of a gel was observed in solution before measurements.

(10,379.0–10,379.5 eV) similar to those of α -GaOOH. Since the first coordination shell of Ga in α -GaOOH corresponds to six oxygens forming a distorted octahedron (Pye et al., 1977), aqueous Ga at acid pH is likely to have a similar environment. By contrast, in Ga-bearing solutions at pH from 2.7 to 5 in the presence of 0.04–0.1 m $\text{SiO}_2(\text{aq})$, the shape and edge-crest position (10,378.3 eV) are distinctly different, resembling those observed in the alkaline solutions. The shift of 1 to 2 eV to the lower energies and the spectral shape are consistent with the change of Ga coordination from 6 to 4 in the presence of silica (Higby et al., 1988; Behrens et al., 1995).

4.2. EXAFS Analysis of Silica-Free Solutions

4.2.1. First atomic shell

Normalized k^2 -weighted EXAFS spectra and their Fourier transforms of selected Si-free solutions at different pH are reported in Figs. 4a and 4b. In strongly acid solutions (pH = 1.1, Ga = 0.001–0.005 m), both EXAFS spectra and their FT exhibit a single contribution from a first shell of oxygens

around Ga. The model of the back transformed signal arising from the first Ga shell (Fig. 6) gives 6 ± 0.5 oxygens with a mean Ga–O distance of $1.95 \pm 0.01 \text{ \AA}$. This is consistent with the presence of the hydrated Ga^{3+} cation, $\text{Ga}(\text{OH}_2)_6^{3+}$, in excellent agreement with previous LAXS (large angle X-ray scattering) and EXAFS studies on concentrated Ga solutions (Ga–O₆ = 1.96 Å, Lindqvist-Reis et al., 1998; Ga–O₆ = 1.95 Å, Michot et al., 2000).

At pH from 2.6 to 4.2, the first coordination sphere of Ga deviates slightly from a regular octahedron, as indicated by an increase of the DW factor (from 0.005 to 0.008, see Table 1). The coordination and average Ga–O distance remain the same within errors as for the strongly acid solutions ($R = 1.94 \pm 0.02 \text{ \AA}$, $N = 5.5 \pm 0.5$). At higher pH (pH ≥ 4.5), however, the Ga–O average distance decreases to about 1.90 Å. This significant bond shortening is accompanied by an increase of DW factors (to ~ 0.01). The examination of the Fourier transform of three successive scans for a 2×10^{-4} m Ga solution at pH 5 reveals significant changes in the form of both first and second Ga shells with time (Fig. 9). In spite of the significant noise

Table 2. Structural parameters of the second and third Ga atomic shells obtained from fitting Ga *K*-edge EXAFS spectra of Ga nitrate solutions with and without aqueous silica.

| Solution composition | | | Atomic pair | <i>R</i> (Å) | <i>N</i> (atom) | σ^2 | chi ² |
|----------------------|-------------|-------------|-------------|--------------|-----------------|------------|------------------|
| pH | m Ga mol/kg | m Si mol/kg | | | | | |
| 1.1 | 0.001 | 0 | n.d. | | | | |
| 1.1 | 0.005 | 0 | n.d. | | | | |
| 2.6 | 0.005 | 0 | Ga–Ga1 | 3.03 | 1.4 | 0.005 | 0.95 |
| | | | Ga–Ga2 | 3.52 | 0.6 | 0.009 | |
| 3.0 | 0.001 | 0 | Ga–Ga1 | 3.04 | 1.1 | 0.006 | 0.70 |
| | | | Ga–Ga2 | 3.47 | 0.6 | 0.004 | |
| 3.6 | 0.001 | 0 | Ga–Ga1 | 3.04 | 3.0 | 0.007 | 0.42 |
| | | | Ga–Ga2 | 3.51 | 1.5 | 0.009 | |
| 4.2 | 0.001 | 0 | Ga–Ga1 | 3.05 | 2.8 | 0.007 | 0.90 |
| | | | Ga–Ga2 | 3.49 | 1.8 | 0.005 | |
| 5.0 | 0.0002 | 0 | Ga–Ga1 | 3.01 | 1.5 | 0.005 | 0.47 |
| | | | Ga–Ga2 | 3.44 | 0.9 | 0.009 | |
| 9.0 | 0.0002 | 0 | n.d. | | | | |
| 9.6 | 0.005 | 0 | n.d. | | | | |
| 9.7 | 0.005 | 0 | n.d. | | | | |
| 2.7 | 0.005 | 0.056 | Ga–Ga | 3.03 | 0.5 | 0.004 | 0.42 |
| | | | Ga–Si | 3.17 | 1.7 | 0.010 | |
| 2.7 | 0.001 | 0.094 | Ga–Si | 3.21 | 1.7 | 0.007 | 0.30 |
| 3.0 | 0.001 | 0.05 | Ga–Si1 | 3.20 | 2.0 | 0.008 | 0.29 |
| | | | Ga–Si2 | 3.41 | 2.0 | 0.008 | |
| 3.6 | 0.001 | 0.044 | Ga–Si1 | 3.17 | 2.0 | 0.007 | 0.42 |
| | | | Ga–Si2 | 3.39 | 2.4 | 0.006 | |
| 4.2 | 0.001 | 0.05 | Ga–Si1 | 3.22 | 2.5 | 0.008 | 0.20 |
| | | | Ga–Si2 | 3.42 | 1.7 | 0.005 | |
| 5.0 | 0.0002 | 0.05 | Ga–Si | 3.20 | 2.5 | 0.009 | 0.33 |
| 8.2 | 0.005 | 0.06 | n.d. | | | | |
| 8.3 | 0.001 | 0.011 | Ga–Si1 | 3.20 | 2.0 | 0.009 | 0.43 |
| | | | Ga–Si2 | 3.43 | 2.0 | 0.009 | |
| 8.5 | 0.001 | 0.011 | Ga–Si1 | 3.16 | 2.4 | 0.008 | 0.26 |
| | | | Ga–Si2 | 3.40 | 2.0 | 0.006 | |
| 9.0 | 0.0002 | 0.01 | Ga–Si1 | 3.17 | 2.8 | 0.009 | 0.52 |
| | | | Ga–Si2 | 3.39 | 2.5 | 0.006 | |
| 9.7 | 0.001 | 0.01 | Ga–Si1 | 3.12 | 2.0 | 0.007 | 0.39 |
| | | | Ga–Si2 | 3.36 | 1.9 | 0.008 | |
| 9.7 | 0.001 | 0.051 | Ga–Si1 | 3.11 | 2.0 | 0.007 | 0.44 |
| | | | Ga–Si2 | 3.35 | 2.0 | 0.007 | |
| 9.7 | 0.005 | 0.05 | n.d. | | | | |
| 10.0 | 0.005 | 0.048 | Ga–Si1 | 3.12 | 2.1 | 0.006 | 0.29 |
| | | | Ga–Si2 | 3.35 | 2.5 | 0.009 | |
| 10.9 | 0.001 | 0.01 | n.d. | | | | |
| α -GaOOH | | | Ga–Ga1 | 2.95 | 2 fix | 0.004 | |
| | | | Ga–Ga2 | 3.24 | 2 fix | 0.006 | 1.63 |
| | | | Ga–Ga3 | 3.41 | 4 fix | 0.009 | |

R = Ga-neighbor mean distance, *N* = Ga coordination number, σ^2 = squared Debye–Waller factor, $\text{chi}^2 = D/(F \times M) \times \Sigma(Y_{\text{exp}}^2 - Y_{\text{fit}}^2)$ (see footnote for Table 1). Typical uncertainties for the determination of *R*, *N* and σ^2 are ± 0.02 Å, ± 0.5 atom for Ga–Si pairs or ± 0.3 atom for Ga–Ga pairs, and ± 0.003 Å², respectively. Fix = value was fixed during fitting; n.d. = second atomic shell was not detected.

affecting these spectra, a broadening of the FT peak corresponding to the Ga first coordination shell, accompanied by a shift to shorter Ga–O distances, can be observed in this figure. The mean first shell Ga–O distance derived from the third scan is 1.88 ± 0.03 Å, which is significantly lower than the Ga–O₆ distance of first Ga shell in more acidic solutions ($R_1 \sim 1.94 \pm 0.03$ Å) or the average Ga–O distance in α -GaOOH solid ($R \sim 1.98$ Å). Consequently, the shorter Ga–O distance suggests the presence of Ga atoms in both sixfold ($R_{\text{Ga-O}_6} \sim 1.95$ Å) and fourfold coordination with oxygens ($R_{\text{Ga-O}_4} \sim 1.83$ Å, see below). However, the short *k* range of this spectrum (from ~ 3 to

~ 14 Å⁻¹) did not permit resolution of such a splitting, instead the least-square fit of the first Ga shell using two Ga–O contributions converged in all cases to a single Ga–O distance (Table 1).

The spectra of *silica-free solutions at basic pH* exhibit a single contribution which corresponds to Ga first shell with four oxygen atoms and Ga–O average distances of 1.83 ± 0.005 Å (Fig. 4, Table 1). This is consistent with the tetrahedral Ga(OH)₄⁻ species which is dominant at pH > 5 in aqueous solution, similar to Al(OH)₄⁻ (Baes and Mesmer, 1976; Bénézeth et al., 1997; Diakonov et al., 1997). The obtained Ga–O

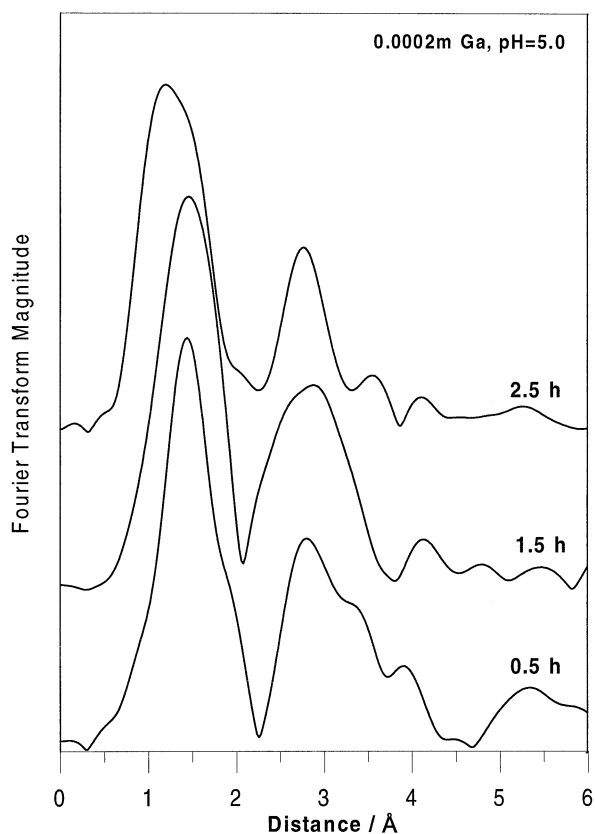


Fig. 9. Evolution of the FT of EXAFS spectra of three successive scans of a 0.0002 molal Ga nitrate solution at pH = 5. The numbers on the figure correspond to the time (in hours) elapsed between the solution preparation and spectra acquisition.

distances are typical for a tetrahedral environment, and in agreement with those found by EXAFS spectroscopy in highly concentrated sodium gallate solutions (Ga–O = 1.80 Å, 0.5 m Ga, Dooryhee et al., 1990), and those for tetrahedral Ga in the framework of Ga-bearing zeolites (Ga–O = 1.78–1.85 Å, Behrens et al., 1995; Fricke et al., 2000), alkali gallosilicate glasses (Ga–O = 1.83 Å, Higby et al., 1988), and β -Ga₂O₃ (Ga–O = 1.83–1.86 Å, Ahman et al., 1996).

4.2.2. Second and third atomic shells

At pH lower than 2, the minor feature observed at 3.5 Å on the FT spectra (Fig. 4b, not corrected for phase shift) might correspond to multiple scattering paths within the symmetrical GaO₆ octahedron (Lindqvist-Reis et al., 1998). At higher pH, this contribution vanishes, and another important second shell feature is observed, with its intensity growing with increasing pH. This feature is similar to that of α -GaOOH, and corresponds to several Ga–Ga pairs with distances ranging from 3.00 to 3.50 Å. The appearance of Ga–Ga contributions clearly demonstrates the formation of Ga polymerized hydroxide complexes. The second shell feature was successfully fitted using two Ga–Ga subshells with distances of $3.01 \leq R_1 \leq 3.04$ and $3.45 \leq R_2 \leq 3.50$ Å (Table 2, Fig. 7). From the analogy with Ga oxy-hydroxide solids whose structures consist of Ga–O/(OH)₆ octahedra sharing their faces ($R_{\text{Ga–Ga}} = 2.84$ Å in

α -Ga₂O₃, Michot et al., 2000), edges ($R_{\text{Ga–Ga}} = 2.95$ – 3.25 Å in α -GaOOH and β -Ga₂O₃, Pye et al., 1977; Ahman et al., 1996) and/or double corners ($R_{\text{Ga–Ga}} = 3.40$ Å in α -GaOOH, Pye et al., 1977), the Ga–Ga distances derived for the hydrolyzed solutions can be attributed to polymeric species with edge and double-corner sharing Ga–O₆ octahedra. These structures found in our dilute solutions are similar to those of Ga(III), Fe(III), and Cr(III) hydroxide polymeric species formed in concentrated solutions (0.2–1.0 mol) during the hydrolysis of nitrate or chloride salts of these metals (Michot et al., 2000; Combes et al., 1989; Bottero et al., 1994; Jolivet et al., 1994). Note that beyond-the-first Ga shells of all hydrolyzed solutions investigated in this study were reasonably fitted using two Ga–Ga contributions at ~ 3.0 and ~ 3.5 Å, in accordance to the degree of freedom for our EXAFS spectra between 4 and 7 (Stern, 1993). The addition of a third Ga–Ga shell (for example, at ~ 3.3 or 3.9 Å) led to highly correlated and often unreasonable Debye–Waller factors and coordination numbers and decreased significantly the goodness-of-fit parameter. Consequently, taking into account the signal-to-noise ratio and k range of the spectra of the dilute solutions investigated in this study, a two-shell model was kept throughout analysis of Ga hydrolysis in acid solutions.

At $2.5 \leq \text{pH} \leq 3$, the numbers of Ga edge-sharing and corner-sharing neighbors ($N_{\text{edge}} = 1.2 \pm 0.2$ and $N_{\text{corner}} = 0.6 \pm 0.3$, respectively) are independent of Ga concentration and close to those found by Michot et al. (2000) for concentrated (~ 0.3 m Ga nitrate) solutions at similar pH. In the pH region 3.5–4.5, the Ga–Ga features are very similar (Fig. 4), and give Ga–Ga distances and number of neighbors of 3.05 ± 0.02 , 3.50 ± 0.02 Å, and 2.9 ± 0.2 , 1.7 ± 0.2 Ga atoms, respectively (see Table 2). Our NMR measurements at $\text{pH} \geq 2.5$ in more concentrated Ga solutions (0.05–0.3 m) clearly show the formation of the Ga₁₃ cation of Keggin-type structure, analogous to Al₁₃. In this structure (Fig. 11), each of the 12 Ga atoms in octahedral coordination “sees” three octahedral neighbors at 3.04 Å linked by edges ($N_{\text{mean}} = 12^{\text{oct}} \times 3/13 = 2.8$) and one central tetrahedral Ga at 3.50 Å ($N_{\text{mean}} = (12^{\text{oct}} \times 1 + 1^{\text{tet}} \times 12)/13 = 1.85$). Thus, the coordination numbers derived in this study strongly suggest that Ga₁₃ is the dominant Ga species at these pH in our dilute solutions. Note that the presence of a single central tetrahedrally coordinated Ga cannot be detected directly from the analysis of the first Ga–O shell: $N_{\text{mean(Ga–O)}}$ would be equal to $(12 \times 6 + 1 \times 4)/13 = 5.85$ in the ideal case of 100% predominance of Ga₁₃ in solution, which is in the limit of the uncertainties (6 ± 0.3) when determining $N_{\text{Ga–O}}$ (see above, and Table 1).

At higher pH (5.0), the Ga–Ga average distances decrease slightly (3.01 and 3.44 Å) which could be attributed to the hydrolysis of the Ga₁₃ cation and formation of precursors of α -GaOOH (Ga–Ga distances = 2.97, 3.23, and 3.40 Å, Pye et al., 1977), which rapidly precipitates at pH around 5. Indeed, the EXAFS spectrum and its Fourier transform for a 2×10^{-4} m Ga solution at pH 5 exhibit additional second-shell contributions and a higher noise than the spectra at lower pH (Figs. 4a and 4b). This can be explained by the rapid kinetics of both transformation of Ga₁₃ and formation of Ga(OH)₃/GaOOH nuclei, which was faster than the time required for a single scan acquisition (~ 50 min). Like the first shell (see above), the second shell of Ga evolves significantly with time (Fig. 9). The

hydrolysis of the Ga_{13} cation with increasing pH and before the precipitation of Ga hydroxides is likely to proceed through the formation of larger polymeric hydroxide complexes in which a part of Ga is tetracoordinated, as suggested from the analysis of the first shell (Sect. 4.2.1). Note, that our NMR spectroscopy measurements at higher Ga concentration (~ 0.1 – 0.2 m) and $\text{pH} > 2.9$ (see above) also suggest the hydrolysis and polymerization of Ga_{13} , and the presence of significant amount of tetracoordinated gallium in the new polycations formed.

4.3. EXAFS Analysis of Silica-Bearing Solutions

4.3.1. First atomic shell

In the presence of aqueous silica at basic pH, the first shell Ga– O_4 distances are distinctly lower (by 0.02 to 0.03 Å) than for their Si-free analogs. This bond shortening can be explained by the replacement of free OH groups in the $\text{Ga}(\text{OH})_4^-$ species by –O– bridges and formation of Ga–O–Si bonds.

In the presence of aqueous silica at acid pH ($2.7 \leq \text{pH} \leq 5.0$) important changes occur in the first coordination shell of gallium. The examination of the EXAFS spectra of Si-bearing solutions reveals distinct amplitude changes and phase shifts in comparison to those for their Si-free analogs (Figs. 4a and 5a). The first shell Ga–O contribution to the Fourier transform (Fig. 5b) is shifted to shorter distances, which is also manifested by a phase shift of its IFT (Fig. 6). The modeling of the first Ga coordination shell (Ga–O) revealed a change in the number of neighbors (4 ± 0.5) and Ga–O distance (1.81 ± 0.01 Å) in comparison to the acid solutions without silica (see above). These parameters are surprisingly close to those found for the first shell of Ga in basic solutions.

At more acid pH ($\text{pH} \sim 2.7$) and moderate Si/Ga ratios (Si/Ga ~ 10), Ga first shell atomic environment was found to be intermediate between those in the polymeric Ga hydroxide species and Ga–silicate complexes at higher pH or Si concentrations. Two Ga–O distances were detected, corresponding to octahedral ($R_1 = 1.94$ Å) and tetrahedral ($R_2 = 1.81$ Å) environment (Table 1). The Ga–O coordination number corresponding to the shorter distance ($N_2 = 1.2$) implies that about 20–25% of Ga is in tetrahedral configuration.

4.3.2. Second and third atomic shells

At basic pH ($\text{pH} \geq 8$), two new distinct contributions (at ~ 2.7 and ~ 3.1 Å, not corrected for phase shift) were detected beyond the first shell (Fig. 5b). Their intensities are independent of Ga concentration, but grow with increasing Si content and decreasing pH (Figs. 10a and 10b), thus suggesting that these contributions arise from silicon atoms in the second coordination shell of gallium. Analysis of this shell was performed using two Ga–Si sets of structural parameters. To diminish the strong correlations between number of neighbors (N) and DW factors, the σ^2 values for both Ga–Si shells were restricted during the fitting to the range 0.002–0.02. These values are typically found at ambient temperature for metal–silicon second shell pairs in zeolites (e.g., Dooryhee et al., 1990) and metal–Si/As/Se pairs in the surface complexes formed during silicate/arsenate/selenate sorption on or coprecipitation with Fe and Cr hydroxides (e.g., Fendorf et al., 1994; Waychunas et al., 1993; Manceau and Charlet, 1994). The high

uncertainties associated with the derived $N_{\text{Ga–Si}}$ values (Table 2) are due to the weak signal arising from the Ga–Si contributions. Nevertheless, this signal is significantly higher than the spectral noise as demonstrated by fits of raw total EXAFS spectra (Fig. 8). It can be seen in this figure that adding two Ga–Si contributions to the fit of raw spectra of Si-bearing solutions considerably improves the fit quality. The influence of MS scattering paths within the Ga– O_4 tetrahedron and Ga–O–Si(O/OH) $_3$ structures, and of the possible presence of the $\text{N}(\text{CH}_3)_4^+$ cation in the outer coordination shell were also tested, but they were found not to contribute to the Ga–Si signal within errors. Reasonable fits were obtained for two Ga–Si contributions with $R_2 = 3.12$ – 3.20 Å, $N_2 = 2.0 \pm 0.5$, and $R_3 = 3.35$ – 3.43 Å, $N_3 = 1.5 \pm 0.5$ (Figs. 7 and 8; Table 2). The first Ga–Si distance is in agreement with that derived by Dooryhee et al. (1990) for Ga–Si pairs in their EXAFS study of Ga–Si alkaline gels ($R_{\text{Ga–Si}} = 3.11$ – 3.14 Å). These Ga–Si distances are very close to those found in crystalline sodium gallozeolites (Dooryhee et al., 1990; Nenoff et al., 1994) implying a similar Ga atomic environment in zeolites and their precursors formed from concentrated Ga–Si alkaline solutions. The second Ga–Si distance ($R_3 = 3.35$ – 3.43 Å) is close to those found by EXAFS spectroscopy in hydrothermally synthesized pentasil silicates (Ga–Si = 3.45–3.50 Å, Okabe et al., 1991). The existence of two different Ga–Si distances is likely to imply formation of two different types of aqueous complexes (see below).

At moderately acid pH ($2.7 \leq \text{pH} \leq 5.0$), the Ga–Ga features observed in the second shell of the SiO_2 -free hydrolyzed Ga solutions, disappear in the presence of aqueous silica (Figs. 5a and 5b). Instead, two new weak features appear at ~ 2.7 and ~ 3.1 Å (not corrected for phase shift), which closely resemble those observed in the Ga–Si basic solutions, thus indicating the presence of analogous Ga–O–Si bonds. The modeling of these features was performed using one or two Ga–Si contributions in the manner similar to that for the basic Si-bearing solutions (see above and Figs. 7 and 8). For 0.05 m Si, 0.001 m Ga solutions at pH 3–4.5 (Si/Ga = 50), two Ga–Si contributions were resolved with $R_2 = 3.20 \pm 0.03$ Å, $N_2 = 2.0 \pm 0.5$, and $R_3 = 3.40 \pm 0.02$ Å, $N_3 = 2 \pm 0.5$. By contrast, in solutions with the highest Si/Ga mole ratio (Si/Ga = 100–250: 0.05 m Si–0.0002 m Ga–pH = 5.0, and 0.094 m Si–0.001 m Ga–pH = 2.7, see Table 2), only a single Ga–Si distance could be resolved ($R_2 \sim 3.20$ Å). This is probably due to both the low Ga–Si signal in our dilute samples, and high structural disorder of Ga sites which attenuates the EXAFS signal. The difficulty in resolving Ga structural environment beyond its first coordination shell by XAFS or NMR spectroscopy has also been demonstrated for Ga–Si concentrated alkaline solutions, gels, glasses and even crystalline zeolites (Behrens et al., 1995; Mortlock et al., 1992).

At more acid pH ($\text{pH} \sim 2.7$) and moderate Si/Ga ratios (Si/Ga = 10), the presence of both Ga–Ga and Ga–Si contributions could be detected beyond the first shell at 3.03 Å and 3.17 Å, respectively (Table 2). The first distance corresponds to Ga octahedra linked by their edges as in Si-free Ga hydrolyzed solutions. Gallium–gallium number of neighbors is however significantly decreased ($N_{\text{edge}} = 0.5$) in comparison to that in the Si-free solutions of the same pH ($N_{\text{edge}} = 1.4$). No Ga–Ga distances at 3.5 Å corresponding to double corner linkages were detected in the presence of Si. The Ga–Si distance of 3.17

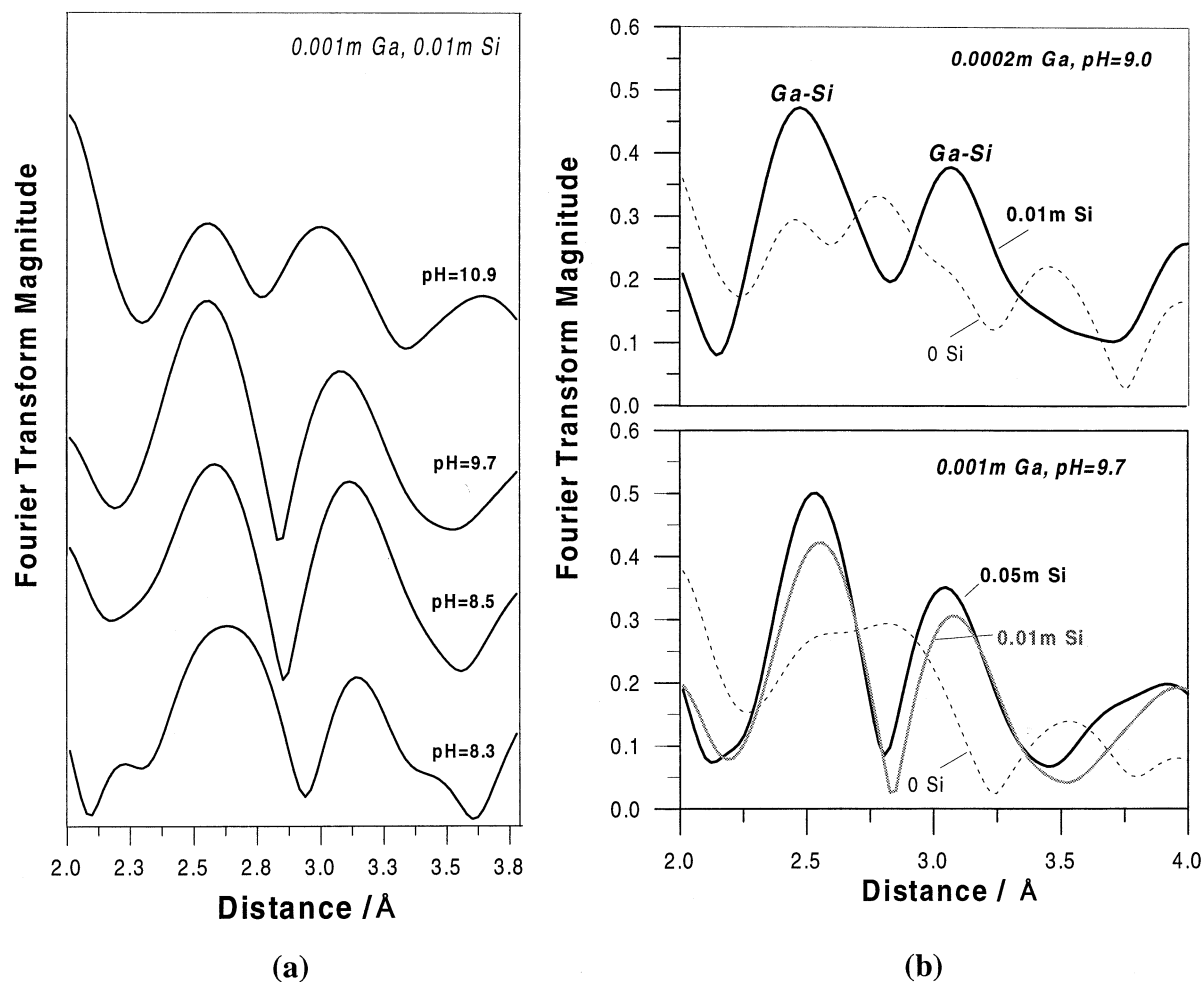


Fig. 10. Evolution of the second coordination shell of Ga shown as the Fourier transform (not corrected for phase shift) of the EXAFS spectra of basic Ga-Si solutions as a function of pH (a), and Ga and Si concentration (b).

Å is also very close to that found in tetrahedral Ga-Si complexes at higher pH. As it was inferred from the analysis of the first shell (Sect. 4.3.1), about 20% of total Ga is present in tetrahedral coordination in this solution. If this ^{141}Ga were entirely complexed with four silicic acid ligands, the overall Ga-Si coordination number would be only 0.8. The experimental value is significantly higher ($N_{\text{Ga-Si}} \sim 1.7 \pm 0.5$), implying that both $^{61}\text{Ga-Si}$ and $^{141}\text{Ga-Si}$ bonds are likely to be present in this solution.

5. DISCUSSION

5.1. Gallium Hydrolysis

The XAFS and NMR results of this study demonstrate that the Ga^{3+} cation rapidly hydrolyzes in dilute aqueous solution via formation of Ga oxy-hydroxide polynuclear species composed of $\text{Ga}(\text{O}/\text{OH}/\text{H}_2\text{O})_6$ octahedra linked together by their edges and double corners. In this respect, Ga hydrolysis is similar to that observed for Fe^{3+} , Cr^{3+} and probably Al^{3+} cations (Baes and Mesmer, 1976; Jolivet et al., 1994). However, some differences in the stoichiometry and species distribution for these M^{3+} cations arise since the early stages of

hydrolysis. At low OH/Ga ratios ($\text{pH} \leq 3.0$) the coordination numbers derived in this study for the Ga-Ga edge ($R_{\text{edge}} = 3.04$ Å) and double corner ($R_{\text{corner}} = 3.50$ Å) linkages ($N_{3.04 \text{ Å}} = 1.1-1.4$, $N_{3.50 \text{ Å}} \sim 0.6$) could imply either the formation of the Ga_{13} polycation (e.g., 30% Ga_{13} + 70% monomeric $\text{Ga}(\text{OH})_n$), or the presence of a mixture of smaller different polymers like edge and double-corner shearing di-, tri-, or tetramers whose schematic structures are represented in Fig. 11. Analogous species were also proposed by Michot et al. (2000) for early stages of Ga hydrolysis in highly concentrated (0.3 m Ga) solutions. Similar polycations were suggested as intermediate species leading to the formation of two types of edge-linked tetramers during the early stages of Cr^{3+} hydrolysis (Jolivet et al., 1994). Small polynuclear species of iron (III) are less stable than their Ga analogs: Fe edge-linked dimers and double-corner trimers rapidly form larger polymers with $\beta\text{-FeOOH}$ -like structures (i.e., “ Fe_{24} ” polycation, Bottero et al., 1994).

For OH/Ga ratios higher than 2, the numbers of Ga neighbors and Ga-Ga distances derived from our EXAFS analysis, together with the NMR signal arising from the Ga- O_4 tetrahedron, clearly demonstrate that the Ga_{13} cation of Keggin-type

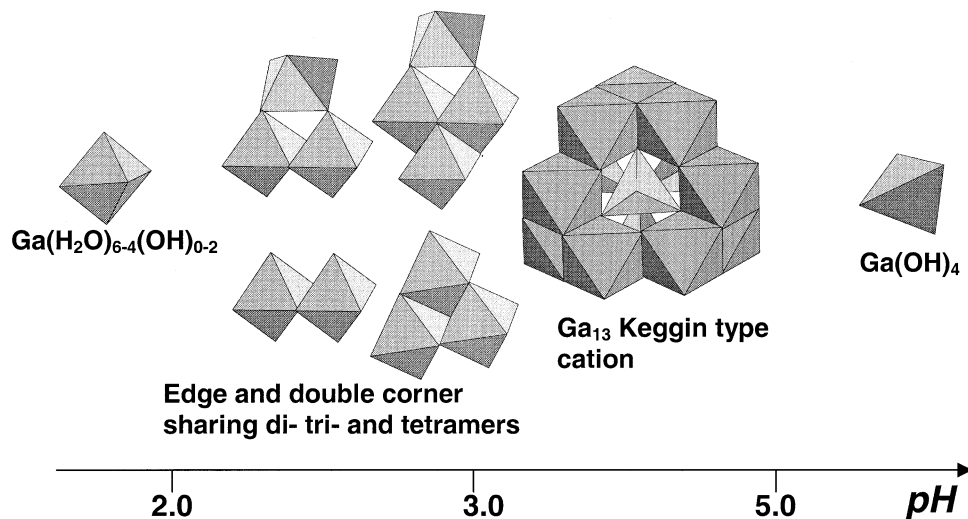


Fig. 11. Schematic structures of Ga hydroxide complexes formed as a function of pH in aqueous solution during Ga^{3+} hydrolysis.

structure is the dominant species in our solutions of low to moderate Ga concentration ($0.0002 \leq m_{\text{Ga}} \leq 0.1$). The Ga_{13} formation was also reported for more concentrated Ga nitrate and chloride solutions at similar hydrolysis ratios (Bradley et al., 1990a, 1990b; Michot et al., 2000).

At pH above 4.5, the Ga_{13} cation seems to transform into more disordered GaOOH-Ga(OH)_3 precursors (see Sect. 4.2.1) which is manifested by the decrease of Ga–Ga number of neighbors and Ga–Ga distances (see Table 2, the 2×10^{-4} Ga solution at pH 5). In this respect, the Ga_{13} polycation is less stable than its aluminum analog which could be isolated in crystalline state by precipitation of basic Al sulfates and selenates at OH/Ga ratios higher than 2 (Johansson, 1962a, 1962b). The rapid transformation of Ga_{13} observed in this study by EXAFS and NMR spectroscopy, respectively, at pH > 4.5 at low Ga concentrations (< 0.001 m) and at pH > 2.9 in more concentrated solutions (≥ 0.1 m), is likely to proceed via the formation of less ordered bigger polymeric species having significant proportions of tetracoordinated Ga with a similar geometry as in Ga_{13} . These polymers are supposed to exist in a very narrow pH range, rapidly forming Ga-hexa-coordinated hydroxide solids. More studies are needed to establish their exact structure and stability. The schematic structures of the Ga hydroxide polymers proposed to form in this study as a function of hydrolysis progress are presented in Fig. 11.

The results of our study on the hydrolysis of $\text{Ga(NO}_3)_3$ dilute solutions can be compared with Ga speciation calculated using thermodynamic data on Ga hydroxide complexes deduced from potentiometric and solubility studies carried out at Ga concentrations below 0.01 m. In Fig. 12 the distribution of Ga hydroxide complexes in a 10^{-3} m Ga solution is calculated as a function of pH at 25 °C. These calculations were performed at ionic strength 0.1, using the equilibrium formation constants for the Ga(OH)_{1-4} mononuclear species from Bénézech et al. (1997), and those for Ga polymers from Baes and Mesmer (1976). The generic formula “ $\text{Ga}_{26}(\text{OH})_{13}^{3+}$ ” was tentatively ascribed by the latter authors to a set of different polymeric species including the Ga_{13} and Ga_{40} polycations which were

detected via potentiometric titrations. It can be seen in Fig. 12 that, in a 10^{-3} m Ga solution, polymeric species begin to form in significant amounts (> 10% of total Ga) above pH 3.5–3.7. Our EXAFS measurements show that, at this pH, Ga speciation is almost entirely dominated by the Ga_{13} species. Thus, the available equilibrium constants for the Ga polymers underestimate significantly their stabilities. Our EXAFS results can therefore help future potentiometric and solubility studies to better quantify the stability of aqueous Ga polymers in dilute solutions.

5.2. Stoichiometry and Structure of Ga–Si Aqueous Complexes

EXAFS and NMR measurements reported in this study demonstrate that aqueous silica forms stable complexes with gallium via the constitution of Ga–O–Si bonds. In these complexes Ga exhibits a tetrahedral atomic environment with oxygens not only at basic and neutral, but also at moderately acid pH, where it is normally hexa-coordinated with oxygens in its hydroxide complexes. The striking similarity of second and third Ga shell atomic environments found by EXAFS spectroscopy in our study implies that similar Ga–silicate complexes form over a wide pH range ($3 \leq \text{pH} \leq 10$). The 3.11–3.20 Å Ga–Si distance determined in the second coordination shell of Ga corresponds to Ga–O–Si bond angles of 125° – 135° and closely resembles Ga atomic environment in zeolite structures where tetrahedral Ga substitutes for silicon (or aluminum) in the zeolite framework rings composed typically of four to six $(\text{Si,Al})\text{O}_4$ tetrahedra (Barrer, 1982; Fricke et al., 2000). It can be thus assumed that these Ga–Si distances correspond to aqueous Ga–Si complexes having a cyclic structure. Cyclic gallosilicate species, which form by exchange of SiO_4 and GaO_4 tetrahedrons in the already existing silica cyclic polymers, were also reported for concentrated Ga–Si solutions using NMR spectroscopy (Mortlock et al., 1992).

The second Ga–Si distance evidenced in this study ($R_2 = 3.39 \pm 0.04$ Å) matches Ga–O–Si angles of $165 \pm 5^\circ$. These

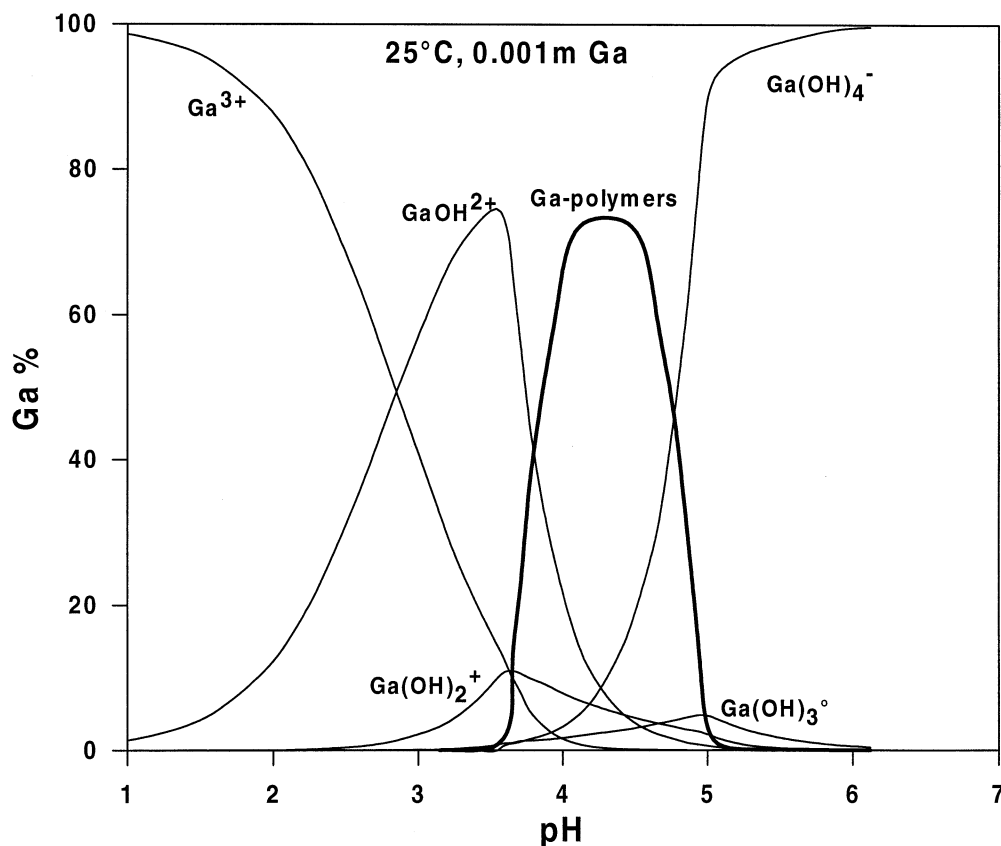


Fig. 12. Distribution of Ga hydroxide species in a 0.001 m Ga nitrate solution as a function of pH at 25 °C. Calculations were performed using the stability constants for Ga species reported by Baes and Mesmer (1976) and Bénézeth et al. (1997).

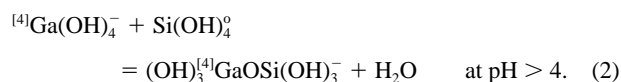
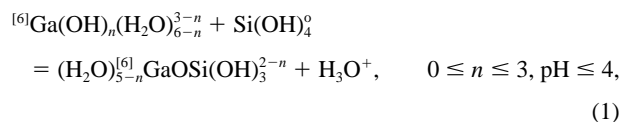
values are likely to correspond to noncyclic, chain-like complexes in which GaO_4 is surrounded by two to four silicate anions. Note that similar di-, tri-, and tetrasilicate complexes were reported using NMR spectroscopy for Al (Q^2_{Al} , Q^3_{Al} , and Q^4_{Al}) in basic solutions with high Si/Al ratios (Kinrade and Swaddle, 1989; Pokrovski et al., 1998). The tentative schematic structures of the Ga-Si complexes found in this study are represented in Figure 13.

Another type of Ga-Si interactions inferred from EXAFS spectra of strongly acid solutions is likely to involve linkages between hexa-coordinated gallium and silicic acid. The Ga-Si distance of 3.17 Å, found in a 0.005 m Ga, 0.056 m Si solution at pH 2.7 (see Sect. 4.3.2), might correspond to silica forming double-corner linkages with two adjacent Ga octahedra. Similar geometries have been found in the case of Fe-Si complexation (Pokrovski et al., 2001) or arsenate and selenate adsorption on Fe-hydroxides (Waychunas et al., 1993; Manceau and Charlet, 1994; Manceau, 1995). More measurements are required however to better quantify this type of Ga-Si interaction in strongly acid solutions.

5.3. Stabilities of Ga-Si Complexes in Natural Waters

The results obtained in this study demonstrate, for the first time, an important effect of silica, at the atomic scale, on the hydrolysis of gallium. Through its complexation with gallium, aqueous silica greatly hampers the formation of Ga polymeric

hydroxide species and thus the precipitation of Ga oxy-hydroxides at pH typical of natural waters (pH > 3). An analogous effect of aqueous silica is observed for Al hydrolysis. For example, polymeric hydroxyaluminosilicate complexes were found to form in significant amounts at ambient temperature in the neutral pH range and serve as precursors for immogolite and allophane formation (Exley and Bishall, 1992, 1993; Xu and Harch, 1993). Moreover, ample evidence exists for Al-Si complex formation in basic solutions in a wide range of Al and Si concentrations (e.g., Guth et al., 1974a, 1974b; 1980; Wada and Wada, 1981; Kinrade and Swaddle, 1989; Gout et al., 2000, references therein). At the low Ga (Al) and Si concentrations of natural waters ($m_{\text{Ga}} < 10^{-6}$ m, $m_{\text{Al}} < 10^{-4}$, $m_{\text{Si}} < 10^{-3}$ m, Bénézeth et al., 1997; Diakonov et al., 1997), both Ga (Al) and Si speciation is entirely dominated by monomeric hydroxide species. The silica linkages with tetrahedral and octahedral Ga, demonstrated in this study, imply two different mechanisms of Si interactions with ^{67}Ga and ^{69}Ga monomeric hydroxide species, respectively,



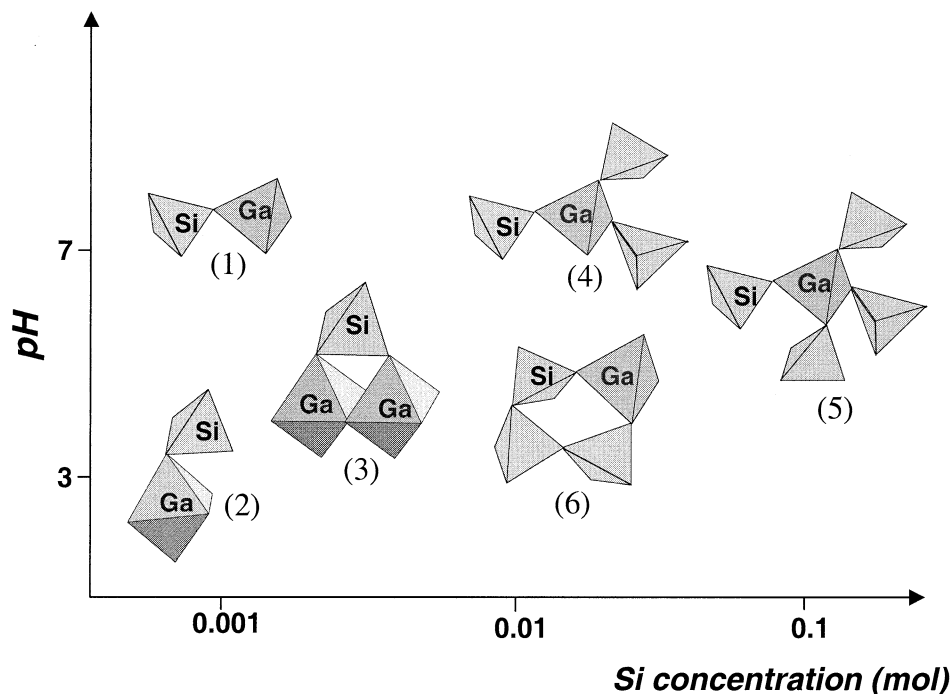


Fig. 13. Schematic structures of Ga-Si complexes proposed in this study from EXAFS and NMR measurements. Complexes (4, 5, 6) were found to form in our experimental solutions at $\text{pH} > 2.7$ and $m_{\text{Si}} > 0.01$ m. Complexes (2 and 3) are likely to form in strongly acid solutions ($\text{pH} < 3$) at moderate Si concentrations ($m_{\text{Si}} < 0.05$ m). Complex (1) is assumed to exist in neutral to basic dilute Si solutions based on the analogy with Al-Si species (Pokrovski et al., 1998).

The proposed reactions are analogous to those recently found for Al-Si interactions in very dilute solutions ($m_{\text{Al,Si}} \leq 0.001$ m), where Al^{3+} and $\text{Al}(\text{OH})_4^-$ form 1:1 complexes with silicic acid, respectively, at acid and basic pH (Pokrovski et al., 1996 and references therein; Pokrovski et al., 1998).

The first reaction is likely to proceed through the substitution of a water molecule by a silicic acid ligand in the first hydration sphere of the hexa-coordinated Ga^{3+} cation (Pokrovski, 1996). This mechanism is similar to that assumed for the hydrolysis of metallic di- and tri-valent cations (Jolivet et al., 1994). The similarity between the mechanisms of formation of hydroxide and silicate complexes in acid solution is illustrated in Fig. 14, where the equilibrium constants of metal-silica complexation reaction (analogous to reaction (1) for $n = 0$) available in the literature for different cations (Na^+ , Ca^{2+} , Mg^{2+} , UO_2^{2+} , La^{3+} , Al^{3+} , Fe^{3+}) are plotted versus their first hydrolysis constants. The good linear correlation (squared correlation coefficient = 0.97) apparent in this figure suggests that both OH^- and $\text{OSi}(\text{OH})_3^-$, which contain negatively charged oxygen donors, form with many metal ions complexes of similar structures and thermodynamics. Similar free energy relationships were demonstrated for many metallic cations between their hydroxide and O-containing organic ligand complexes in aqueous solution (Martell and Hancock, 1996), or complexes adsorbed on oxy-hydroxide mineral surfaces (Stumm, 1992). The linear relationship presented in our study allows estimation of the stability of metal-silicate complexes for which there are no available data. The equilibrium constant at 25 °C for reaction (1) between Ga^{3+} and silicic acid can be thus estimated from the above correlation and using the first hydrolysis constant of

Ga^{3+} from Bénézeth et al. (1997): $\log K_1^{\text{Si}} = -0.7 \pm 0.2$. Speciation calculations carried out using this constant indicate that the $\text{GaOSi}(\text{OH})_3^{2+}$ complex can account for only 10% to 15% of the total Ga at pH between 3 and 4 in the presence of 30 ppm of aqueous silica.

Complexes between the monomeric hydroxide species (GaOH^{2+} , $\text{Ga}(\text{OH})_2^+$, and $\text{Ga}(\text{OH})_3^0$) and silicic acid are expected to be even weaker than that with Ga^{3+} because the decrease of species charge should diminish metal-silica electrostatic attractions. This has been verified for $\text{Al}(\text{OH})_n$ -acetate complexes (Bénézeth et al., 1994) and for $\text{Al}(\text{OH})_{1-3}$ -silicate complexes in which Al exists in sixfold coordination (Pokrovski et al., 1996; Salvi et al., 1998). Thus, by analogy with Al, silica complexes with the intermediate hydrolyzed Ga species in coordination 6 can be assumed to be negligible at silica concentrations of natural waters.

The formation of stable silicate species with gallium in fourfold coordination as demonstrated in this study, implies that, like for Al, Ga-Si complexation is much stronger when the metal takes the tetrahedral coordination. This is consistent with the formation of Ga-O-Si covalent bonds, similar to those observed for Al-Si complexes. The percentage of complexed Ga and the number of silicate ligands can be qualitatively related to the intensities of Ga-Si contributions to the Fourier transforms of EXAFS spectra obtained in this study. In Ga-Si bearing alkaline solutions, these intensities increase with decreasing pH from 11 to 8 at the same silica concentration (Fig. 10a). This evolution of the stability of Ga-Si complexes with pH is very similar to that observed for Al-Si complexes from potentiometric and NMR (Pokrovski et al., 1998), and Raman

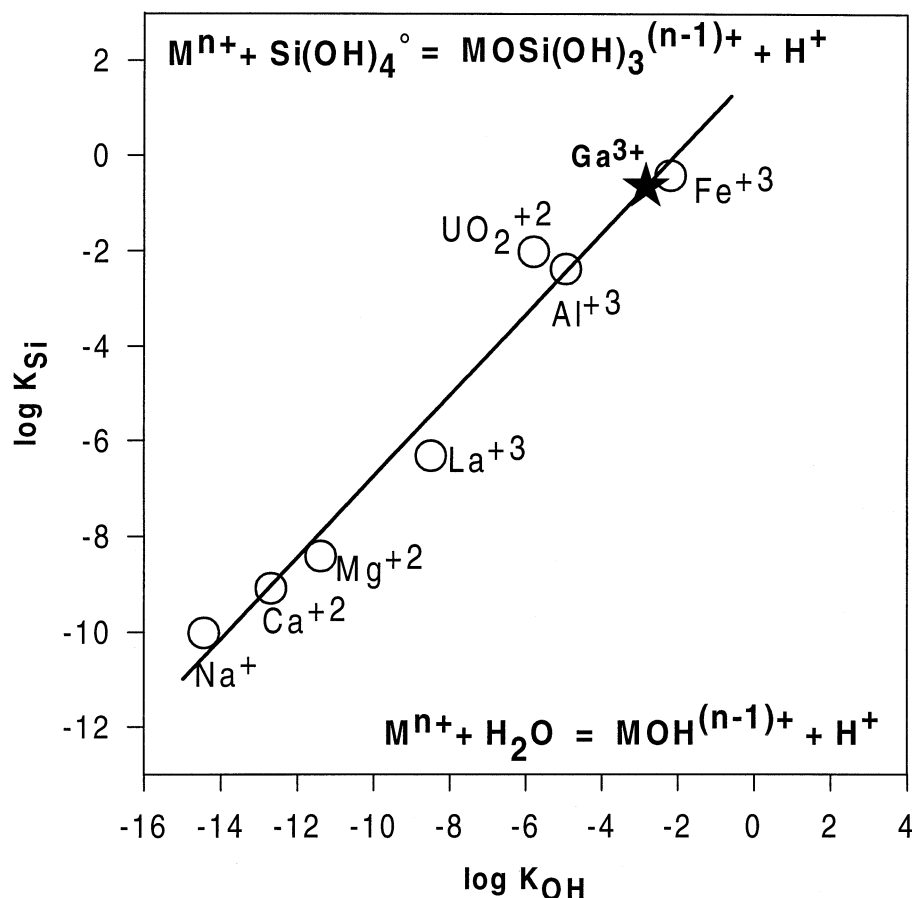


Fig. 14. Logarithm of the complex formation constant between a metal cation and aqueous silicic acid (K_{Si}) as a function of the logarithm of the first hydrolysis constant of the metal (K_{OH}) at 25 °C. Stability constants of metal-silica complexes were taken from Sillen and Martell (1964) for Na, Santschi and Schindler (1974) for Ca and Mg, Pokrovski for La, Pokrovski et al. (1996) for Al, Satoh and Chopin (1992) for UO_2^{2+} , and Weber and Stumm (1965) and Olson and Melia (1973) for Fe. The hydrolysis constants for the metals were taken from Baes and Mesmer (1976). The circles stand for the data for corresponding cation, but the solid line represents a linear regression of these data: $\log K_{Si} = 0.85 \log K_{OH} + 1.8$ ($R^2_{xy} = 0.97$). The star denotes Ga^{3+} cation for which $\log K_{Si}$ was determined from the above correlation using the Ga^{3+} first hydrolysis constant from Bénézeth et al. (1997).

spectroscopy measurements (Gout et al., 2000). By analogy with aluminum, it can be suggested that, at the low silica and gallium concentrations of natural waters, the dimeric complex between $Ga(OH)_4^-$ and silicic acid formed according to reaction (2) should be most probable. In the absence of data for metals other than Al, it is however difficult to quantify the stability of this ^{14}Ga -Si species. If we assume, in the first approximation, that the equilibrium constant of reaction (2) for $Ga(OH)_4^-$ is equal to that of the analogous reaction with $Al(OH)_4^-$ ($\log K_2^{Al} = 3.7 \pm 0.2$ at 25 °C, Pokrovski et al., 1998), the $(OH)_3GaOSi(OH)_3^-$ complex would account for about 90% of total Ga in the pH range from 4.5 to 10, for silica-rich soil solutions and waters from tropical watersheds (~20–30 ppm Si, Viers et al., 1997). Taking account of the easier tendency of Ga than Al to pass in tetrahedral coordination with increasing pH (above pH 4 and 7 for Ga and Al, respectively), Ga-Si complexes might be even more important than their Al analogs. More work is however needed to quantify their stabilities in dilute natural fluids. The results of our study imply that explicit account for Ga-Si complexing should be done when analyzing

Ga mobility in surficial waters and the incorporation of this trace metal in clays and iron and aluminum oxy-hydroxides.

6. CONCLUDING REMARKS

The results obtained in this study showed that Ga(III) hydrolysis in dilute solutions proceeds at early stages via formation of ^{61}Ga polynuclear hydroxide complexes in which GaO_6 octahedra share common corners and edges, which is similar to Fe(III), Al, and Cr(III) hydrolysis. As hydrolysis progresses, these species are rapidly replaced by the Ga_{13} polycation, structurally similar to Al_{13} , which becomes the dominant species at OH/Ga ratios (R) of ~2. At higher R , and just before the Ga-hydroxide precipitation, both EXAFS and NMR measurements provide evidence that larger, less ordered, polynuclear Ga species with significant proportions of ^{14}Ga form at the expense of Ga_{13} . This new feature has not been observed for other M^{3+} cations like Al, Cr or Fe. At later hydrolysis stages ($R > 3.5$), Ga, like Al, exhibits a tetrahedral coordination

corresponding to the dominant $\text{Ga}(\text{OH})_4^-$ species, in agreement with previous studies.

Important changes in Ga hydrolysis have been detected in the presence of aqueous silica. Gallium is tetra-coordinated both in basic and acid solutions ($\text{pH} \geq 3$), and forms stable gallium–silicate complexes in which it binds via oxygen bridges to $\sim 2 \pm 1$ silicons at $3.16 \pm 0.05 \text{ \AA}$, and $\sim 2 \pm 1$ silicons at $3.39 \pm 0.03 \text{ \AA}$. This Ga atomic environment is likely to correspond to cyclic Ga-Si_{2-3} and chain-like GaSi_{2-4} species, formed via covalent Ga–O–Si bonds. At very acid pH (< 2.8) and moderate silica concentrations, the presence of another type of Ga–Si complex, in which Ga remains hexa-coordinated and binds to silicon tetrahedra via the GaO_6 octahedron corners, has been also detected. The evolution of both ^{67}Ga - and ^{69}Ga -silicate complexes with pH and Si concentration is similar to that for the analogous Al–Si species (Pokrovski et al., 1998; Salvi et al., 1998). This analogy allows, for the first time, estimation of the stabilities of the simplest Ga–Si complexes which are likely to form in dilute natural solutions. Equilibrium calculations using the derived stability constants for the $^{67}\text{GaOSi}(\text{OH})_3^{2+}$ and $^{69}\text{Ga}(\text{OH})_3\text{OSi}(\text{OH})_3^-$ complexes analogous to those formed by Al in very dilute solutions, indicate that, as for aluminum, silicic acid greatly hampers Ga hydrolysis and enhances Ga mobility in natural waters.

The similarity of Ga and Al hydrolysis and interactions with aqueous silica demonstrated in this study provides new insights for understanding aluminosilicate precipitation and trace element incorporation into solid phases in surficial aquatic environments. Polymeric Ga–Si and Al–Si complexes formed from supersaturated solutions could be viewed as precursors for the formation of Al/Ga-bearing minerals. Different proportions of ^{67}Al to ^{69}Al observed in secondary aluminosilicates are likely to reflect, at least partially, the amount and structures of Al–Si complexes existing in the solution from which these solids have precipitated.

The combination of XAFS and NMR spectroscopy was shown to have great potential in deciphering the processes of metal hydrolysis/condensation and complexation in aquatic media. Ab initio quantum mechanics calculations can be also effectively coupled with these in situ spectroscopic methods to help constrain the structures and stabilities of aqueous species. Work is currently in progress to quantify Al–Si and Fe(III)–Si interactions in dilute aqueous solution using this combined approach.

Acknowledgments—We are grateful to the IF CRG commission of the ESRF (Grenoble) for providing beamtime and access to the synchrotron facility. We would like to thank Yvonne Soldo, Olivier Proux, and Jean-Jacques Menthonnex for their generous help and professional assistance during XAFS measurements at BM 32 beamline of the ESRF. Daniel Aberdam and Marcus Winterer are thanked for providing us with their programs for XAFS treatment (SEDEM and XAFS, respectively). We are grateful to Marc Vedrenne who performed NMR measurements. We are indebted to Jacques Roux for his great help with software installation and running, and Jean-Michel Bény for his advice on crystallography. Insightful comments by the Associate Editor, David Wesolowski, and three anonymous reviewers greatly improved the presentation and clarity of this paper.

Associate editor: D. J. Wesolowski

REFERENCES

- Aberdam D. (1998) SEDEM, a software package for EXAFS extraction and modelling. *J. Synchrotron Rad.* **5**, 1287–1297.
- Ahman J., Svensson G., and Albertsson J. (1996) A reinvestigation of β -gallium oxide. *Acta Crystallogr. C* **52**, 1336–1338.
- Akitt J. W., Greenwood N. N., Khandelwal B. L., and Lester G. D. (1972) ^{27}Al nuclear magnetic resonance studies of the hydrolysis and polymerisation of the hexa-aquo-aluminum(III) cation. *J. Chem. Soc. Dalton Trans.* **1972**, 604–610.
- Akitt J. W. and Elders J. M. (1988) Multinuclear magnetic resonance studies of the hydrolysis of aluminum (III). Part 8. Base hydrolysis monitored at very high magnetic field. *J. Chem. Soc. Dalton Trans.* 1347–1355.
- Ankudinov A. L. and Rehr J. J. (1997) Relativistic spin-dependent X-ray absorption theory. *Phys. Rev. B* **56**, R1712–R1715.
- Baes C. F. Jr. and Mesmer R. E. (1976). *The Hydrolysis of Cations*. Wiley.
- Barrer R. M. (1982) *Hydrothermal Chemistry of Zeolites*. Academic.
- Bénézech P., Castet S., Dandurand J.-L., Gout R., and Schott J. (1994) Experimental study of aluminum–acetate complexing between 60 and 200 °C. *Geochim. Cosmochim. Acta* **58**, 4561–4571.
- Bénézech P., Diakonov I., Pokrovski G. S., Dandurand J.-L., Schott J., and Khodakovskiy I. L. (1997) Gallium speciation in aqueous solution. Experimental study and modelling. Part II. Solubility of α -GaOOH in acidic solutions from 150 to 250 °C and hydrolysis constants of gallium (III) to 300 °C. *Geochim. Cosmochim. Acta* **61**, 1345–1357.
- Behrens P., Kosslick H., Tuan V. A., Fröba M., and Niessendorfer F. (1995) X-ray absorption spectroscopic study on the structure and crystallization of Ga-containing MFI-type zeolites. *Microporous Mater.* **3**, 433–441.
- Birchall J. D., Exley C., Chappell J. S., and Phillips M. J. (1989) Acute toxicity of aluminium to fish eliminated in silicon-rich acid waters. *Nature* **338**, 146–148.
- Bonnin D., Calas G., Suquet H., and Pezerat H. (1985) Site occupancy of Fe^{3+} in Galfeld nontronite: a spectroscopic study. *Phys. Chem. Miner.* **12**, 55–64.
- Bottero J. Y., Manceau A., Villieras F., and Tchoubar D. (1994) Structure and mechanisms of formation of $\text{FeOOH}(\text{Cl})$ polymers. *Langmuir* **10**, 316–319.
- Bradley S. M., Kydd R. A., Yamdagni R. (1990b) Detection of a new polymeric species formed through the hydrolysis of gallium (III) salt solutions. *J. Chem. Soc. Dalton Trans.*, 413–417.
- Bradley S. M., Kydd R. A., and Yamdagni R. (1990a) Study of the hydrolysis of combined Al^{3+} and Ga^{3+} aqueous solutions: Formation of an extremely stable $\text{GaO}_4\text{Al}_{12}(\text{OH})_{24}(\text{H}_2\text{O})_{12}^{7+}$ polyoxycation. *Magn. Res. Chem.* **28**, 746–750.
- Browne B. A. and Driscoll C. T. (1992) Soluble aluminum silicates: stoichiometry, stability, and implications for environmental geochemistry. *Science* **256**, 1667–1670.
- Combes J. M., Manceau A., Calas G., and Bottero J. Y. (1989) Formation of ferric oxides from aqueous solutions: A polyhedral approach by X-ray absorption spectroscopy: I. Hydrolysis and formation of ferric gels. *Geochim. Cosmochim. Acta* **53**, 583–594.
- Crosier E. D., Rehr J. J., and Ingalls R. (1988) Amorphous and liquid systems. In *X-ray Absorption. Principles, Applications, Techniques of EXAFS, SEXAFS and XANES* (ed. D. C. Koningsberger and R. Prins). pp. 373–442. Wiley-Interscience.
- Decarreau A., Bonnin D., Badaut-Trauth D., Couty R., and Kaiser P. (1987) Synthesis and crystallography of ferric smectite by evolution of Si–Fe coprecipitates in oxidizing conditions. *Clay Minerals* **22**, 207–223.
- Diakonov I., Pokrovski G. S., Bénézech P., Schott J., Dandurand J.-L., and Escalier J. (1997) Gallium speciation in aqueous solution. Experimental study and modelling. Part I. Thermodynamic properties of $\text{Ga}(\text{OH})_4^-$ to 300 °C. *Geochim. Cosmochim. Acta* **61**, 1333–1343.
- Doelsch E., Rose J., Masion A., Bottero J.Y., Nahon D., and Bertsch P. M. (2000) Speciation and crystal chemistry of iron (III) chloride hydrolyzed in the presence of SiO_4 ligands. 1. An Fe K-edge EXAFS study. *Langmuir* **16**, 4726–4731.
- Dooryhee E., Greaves G. N., Steel A. T., Townsend R. P., Carr S. W., Thomas J. M., and Catlow C. R. A. (1990) Structural studies of

- high-area zeolitic adsorbents and catalysts by a combination of high-resolution X-ray powder diffraction and X-ray absorption spectroscopy. *Faraday Discuss. Chem. Soc.* **89**, 119–136.
- Exley C. and Birchall J. D. (1992) Hydroxyaluminosilicate formation in solutions of low aluminium concentration. *Polyhedron* **11**, 1901–1907.
- Exley C. and Birchall J. D. (1993) A mechanism of hydroxyaluminosilicate formation. *Polyhedron* **12**, 1007–1017.
- Farges F. (1996) Does Zr-F complexation occur in magmas? *Chem. Geol.* **127**, 253–268.
- Farges F., Brown G. E. Jr., and Rehr J. J. (1996a) Coordination chemistry of Ti(IV) in silicate glasses and melts: I. XAFS study of titanium coordination in oxide model compounds. *Geochim. Cosmochim. Acta* **60**, 3023–3038.
- Farges F., Brown G. E. Jr., Navrotsky A., Gan H., and Rehr J. J. (1996b) Coordination chemistry of Ti(IV) in silicate glasses and melts: III. Glasses and melts from ambient to high temperatures. *Geochim. Cosmochim. Acta* **60**, 3055–3065.
- Farmer V. C., Fraser A. R., and Tait J. M. (1977) Synthesis of imolomite: a tubular aluminosilicate polymer. *J. Chem. Soc. Chem. Comm.* **1977**, 462–463.
- Farmer V. C., Fraser A. R., and Tait J. M. (1979) Characterization of the chemical structures of natural and synthetic aluminosilicate gels and sols by infrared spectroscopy. *Geochim. Cosmochim. Acta* **43**, 1417–1420.
- Farmer V. C. and Lumsdon D. G. (1994) An assessment of complex formation between aluminium and silicic acid in acidic solutions. *Geochim. Cosmochim. Acta* **58**, 3331–3334.
- Faust B. C., Labiosa W. B., Dai K. H., MacFall J. S., Browne B. A., Ribeiro A. A., and Richter D. D. (1995) Speciation of aqueous mononuclear Al(III)-hydroxo and other Al(III) complexes at concentrations of geochemical relevance by ^{27}Al nuclear magnetic resonance spectroscopy. *Geochim. Cosmochim. Acta* **59**, 2651–2661.
- Fendorf S. E., Lamble G. M., Stapleton M. G., Kelley M. J., and Sparks D. L. (1994) Mechanisms of chromium (III) sorption on silica. I. Cr(III) surface structure derived by extended X-ray absorption fine structure spectroscopy. *Environ. Sci. Technol.* **28**, 284–289.
- Fricke R., Kosslick H., Lischke G., and Richter M. (2000) Incorporation of gallium into zeolites: Syntheses, properties and catalytic application. *Chem. Rev.* **100**, 2303–2405.
- Gout R., Pokrovski G. S., Schott J., and Zwick A. (1999) A Raman spectroscopy study of aluminum-silica complexing in aqueous solution. *J. Sol. Chem.* **28**, 73–82.
- Gout R., Pokrovski G. S., Schott J., and Zwick A. (2000) Raman spectroscopic study of aluminum silicate complexing at 20 °C in basic solutions. *J. Sol. Chem.* **29**, 1173–1186.
- Guth J-L., Caultet P., and Wey R. (1974a) Contribution à l'étude du mécanisme de formation des zéolites. I. Mise en évidence de complexes aluminosilicates solubles par acidimétrie. *Bull. Soc. Chim. Fr.* **1974**, 1758–1762.
- Guth J-L., Caultet P., and Wey R. (1980) Contribution à l'étude du mécanisme de formation des zéolites. II. Mise en évidence de complexes aluminosilicates solubles par conductométrie. *Bull. Soc. Chim. Fr.*, 2363–2366.
- Guth J-L., Caultet P., Jacques P., and Wey R. (1980) Contribution à l'étude du mécanisme de formation des zéolites. IV. - Mise en évidence de complexes aluminosilicates dans des solutions aqueuses basiques contenant des cations sodium par spectroscopie Raman-Laser. *Bull. Soc. Chim. Fr.*, 121–126.
- Higby P. L., Shelby J. E., Phillips J. C., and Legrand A. D. (1988) EXAFS study of alkali gallosilicate glasses. *J. Non-Cryst. Solids* **105**, 139–148.
- Johanson G. (1962a) On the crystal structure of the basic aluminum sulfate $13\text{Al}_2\text{O}_3 \cdot 6\text{SO}_3 \cdot x\text{H}_2\text{O}$. *Ark. Kemi* **20**, 321–342.
- Johanson G. (1962b) The crystal structures of $[\text{Al}_2(\text{OH})_2(\text{H}_2\text{O})_8](\text{SO}_4)_2 \cdot 2\text{H}_2\text{O}$ and $[\text{Al}_2(\text{OH})_2(\text{H}_2\text{O})_8](\text{SeO}_4)_2 \cdot 2\text{H}_2\text{O}$. *Acta Chem. Scand.* **16**, 403–420.
- Jolivet J-P., Henry M., and Livage J. (1994) *De la Solution à l'Oxyde*. InterEditions and CNRS Editions.
- Kinrade S. D. and Swaddle T. W. (1989) Direct detection of aluminosilicate species in aqueous solution by silicon-29 and aluminum-27 NMR spectroscopy. *Inorg. Chem.* **28**, 1952–1954.
- Konhäuser K. O. and Ferris F. G. (1996) Diversity of iron and silica precipitation by microbial mats in hydrothermal water, Iceland: Implications for Precambrian iron formations. *Geology* **24**, 323–326.
- Koroleff F. (1976) Determination of silicon. In *Methods of Seawater Analysis* (ed. K. Grasshoff). Springer-Verlag.
- Lindqvist-Reis P., Munoz-Paez A., Diaz-Moreno S., Pattanaik S., Parson I., and Sandstrom M. (1998) The structure of the hydrated Ga(III), In(III) and Cr(III) ions in aqueous solutions. A large angle X-ray scattering and EXAFS study. *Inorg. Chem.* **37**, 6675–6683.
- Manceau A. and Charlet L. (1994) The mechanism of selenate adsorption on goethite and hydrous ferric oxide. *J. Colloid. Interface Sci.* **168**, 87–93.
- Manceau A. (1995) The mechanism of anion adsorption on iron oxides: Evidence for the bonding of arsenate tetrahedra on free $\text{Fe}(\text{O},\text{OH})_6$ edges. *Geochim. Cosmochim. Acta* **59**, 3647–3653.
- Martell A. E. and Hancock R. D. (1996) *Metal Complexes in Aqueous Solutions*. Plenum.
- Mayer T. D. and Jarrell W. M. (1996) Formation and stability of iron(II) oxydation products under natural concentrations of dissolved silica. *Water Res.* **30**, 1208–1214.
- Michot L. J., Montargès-Pelletier E., Lartiges B. S., d'Espinose de la Caillerie J-B., and Briois V. (2000) Formation mechanism of the Ga_{13} Keggin ion: A combined EXAFS and NMR study. *J. Am. Chem. Soc.* **122**, 6048–6056.
- Mortlock R. F., Bell A. T., and Radke C. J. (1992) ^{29}Si and ^{71}Ga NMR investigations of alkylammonium gallosilicate solutions. *J. Phys. Chem.* **96**, 2968–2975.
- Nenoff T. M., Harrison W. T. A., Gier T. E., Keder N. L., Zaremba C. M., Srdanov V. I., Nicol J. T., and Stucky G. D. (1994) Structural and chemical investigations of $\text{Na}_3(\text{ABO}_4)_3 \cdot 4\text{H}_2\text{O}$ -type sodalite phases. *Inorg. Chem.* **33**, 2472–2480.
- Okabe K., Matsubayashi N., Sayama K., Arakawa H., and Nishijima A. (1991) EXAFS investigation of pentasil-structured gallium-containing metallosilicates. *Bull. Chem. Soc. Jpn.* **64**, 2602–2604.
- Öhman L-O. and Edlund U. (1996) Aluminum-27 NMR of solutions. In *Encyclopedia of NMR* (eds. D. M. Grant and R.K. Harris), pp. 742–751. Wiley.
- Olson L. L. and O'Melia C. R. (1973) The interactions of Fe(III) with $\text{Si}(\text{OH})_4$. *J. Inorg. Nucl. Chem.* **35**, 1977–1985.
- Pokrovski G. S. (1996) Etude expérimentale du comportement du germanium, du silicium et de l'arsenic et de la complexation de l'aluminium avec la silice dans les solutions naturelles. Thèse de Doctorat de l'Université Paul-Sabatier.
- Pokrovski G. S. and Schott J. (1998) Experimental study of the complexation of silicon and germanium with aqueous organic species. Implications for Ge and Si transport and the Ge/Si ratio in natural waters. *Geochim. Cosmochim. Acta* **62**, 3413–3428.
- Pokrovski G. S., Martin F., Hazemann J-L., and Schott J. (2000) An X-ray absorption fine structure spectroscopy study of germanium-organic ligand complexes in aqueous solution. *Chem. Geol.* **163**, 151–165.
- Pokrovski G. S., Schott J., Harrichoury J-C., and Sergeev A. S. (1996) The stability of aluminum silicate complexes in acidic solutions from 25 to 150 °C. *Geochim. Cosmochim. Acta* **60**, 2495–2501.
- Pokrovski G. S., Schott J., Hazemann J-L., Martin F., Farges F., and Pokrovsky O.S. (2001) An X-ray absorption fine structure spectroscopy study of iron(III)-silica and gallium-silica complexes in aqueous solution: Implications for the hydrolysis and the formation of iron and aluminum oxy-hydroxides and silicates. *European Union of Geosciences-XI. April 2001. Journal of Conference Abstracts on CD-Rom, Vol. 6, No. 1.*
- Pokrovski G. S., Schott J., Salvi S., Gout R., and Kubicki J. D. (1998) Structure and stability of aluminosilicate complexes in neutral to basic solutions. Experimental study and molecular orbital calculations. *Min. Mag.* **62A**, 1194–1196.
- Press W. H., Flannery B. P., Teukolsky S. A., and Vetterling W. T. (1986) *Numerical Recipes-The Art of Scientific Computing*. Cambridge University Press.
- Pye M. F., Birtill J. J., and Dickens P. G. (1977) α -Gallium oxide deuteriohydroxide: A power neutron diffraction investigation. *Acta Crystallogr. B.* **33**, 3224–3226.

- Salvi S., Pokrovski G. S., and Schott J. (1998) Experimental investigation of aluminum–silica aqueous complexing at 300 °C. *Chem. Geol.* **151**, 51–67.
- Santschi P. H. and Schindler P. W. (1974) Complex formation in the ternary systems Ca–H₄SiO₄–H₂O and Mg–H₄SiO₄–H₂O. *J. Chem. Soc. Dalton Trans.*, 181–184.
- Satoh I. and Choppin G. R. (1992) Interaction of uranyl (VI) with silicic acid. *Radiochim. Acta* **56**, 85–87.
- Sillen L. G. and Martell A. E. (1976) *Stability Constants of Metal-Ion Complexes: Special Publication No. 17*. The Chemical Society.
- Schwertmann U. and Thalmann H. (1976) The influence of Fe(II), Si, and pH on the formation of lepidocrocite and ferrihydrite during oxidation of aqueous FeCl₂ solutions. *Clay Miner.* **11**, 189–200.
- Soldo Y., Hazemann J. L., Aberdam D., Inui M., Tamura K., Raoux D., Pernot E., Jal J. F., and Dupuy-Philon J. (1998) Semiconductor-to-metal transition in fluid selenium at high pressure and temperature: An investigation using X-ray absorption spectroscopy. *Phys. Rev. B* **57**, 258–268.
- Stern E. A. (1993) Number of relevant independent points in x-ray-absorption fine-structure spectra. *Phys. Rev. B* **48**, 9825–9827.
- Stumm W. (1992) *Chemistry of the Solid-Water Interface*. Wiley.
- Teo B. K. (1986) *EXAFS: Basic Principles and Data Analysis*. Inorganic Chemistry Concepts 9. Springer-Verlag.
- Thomas F., Masion A., Bottero J. Y., Rouiller J., Montigny F., and Génévier F. (1993) Aluminum (III) speciation with hydroxy carboxylic acids. ²⁷Al NMR study. *Environ. Sci. Technol.* **27**, 2511–2516.
- Vempati R. K. and Loeppert R. H. (1989) Influence of structural and adsorbed Si on the transformation of synthetic ferrihydrite. *Clays Clay Miner.* **37**, 273–279.
- Viers J., Dupré B., Polve M., Schott J., Dandurand J.-L., and Braun J.-J. (1997) Chemical weathering in the drainage basin of a tropical watershed (Nsimi-Zoétéélé site, Cameroon): comparison between organic-poor and organic-rich waters. *Chem. Geol.* **140**, 181–206.
- Wada S.-I. and Wada K. (1981) Reactions between aluminate ions and orthosilicic acid in dilute, alkaline to neutral solutions. *Soil Sci.* **132**, 267–273.
- Waychunas G. A., Rea B. A., Fuller C. C., and Davis J. A. (1993) Surface chemistry of ferrihydrite: Part I. EXAFS studies of the geometry of coprecipitated and adsorbed arsenate. *Geochim. Cosmochim. Acta* **57**, 2251–2269.
- Weber W. and Stumm W. (1965) Formation of a silicato-iron (III) complex in dilute aqueous solutions. *J. Inorg. Nucl. Chem.* **27**, 237–239.
- Wesolowski D. J., Palmer D. A., and Mesmer R. E. (1995) Measurements and control of pH in hydrothermal solutions. In *Water-Rock Interaction* (eds. Y. K. Kharaka and O. V. Chudakov), pp. 51–55. Balkema.
- Winters G. V. and Buckley D. E. (1986) The influence of dissolved FeSi₃O₅(OH)₈ on chemical equilibria in pore waters from deep sea sediments. *Geochim. Cosmochim. Acta* **50**, 277–288.
- Winterer M. (1997) XAFS a data analysis program for material sciences. *J. Physique IV* **7**, C2–243 (Abstr).
- Xu S. and Harsh J. B. (1993) Labile and nonlabile aqueous silica in acid solutions: Relation to the colloidal fraction. *J. Soil Sci. Soc. Am.* **57**, 1271–1277.
- Zabinky S. Y., Rehr J. J., Ankudinov A. L., Albers R. S., and Eller M. J. (1995) Multiple scattering calculations of X-ray absorption spectra. *Phys. Rev. B* **52**, 2995–3009.